2021-12-01

Human endogenous retrovirus type K promotes proliferation and confers sensitivity to anti-retroviral drugs in Merlin-negative schwannoma and meningioma.

Maze, EA

http://hdl.handle.net/10026.1/18487

Human endogenous retrovirus type K promotes proliferation and confers sensitivity to anti-retroviral drugs in Merlin-negative schwannoma and meningioma.

Emmanuel A. Maze[2†], Bora Agit[1†], Shona Reeves[1], David A. Hilton[1], David B. Parkinson[1], Liyam Laraba[1], Emanuela Ercolano[1], Kathreena M. Kurian[4], C. Oliver Hanemann[1+], Robert Belshaw [2,3+*] and Sylwia Ammoun[1+*]

[1]Faculty of Health: Medicine, Dentistry and Human Sciences, Plymouth University, UK

[2]School of Biomedical Sciences, Faculty of Health: Medicine, Dentistry and Human Sciences, University of Plymouth, UK

[3]Department of Biology, College of Science and Technology, Wenzhou-Kean University, Wenzhou, Zhejiang Province, China.

[4]Institute of Clinical Neuroscience, University of Bristol and Southmead Hospital - North Bristol Trust, Bristol, UK.

[+,†]These authors contributed equally

Running title: HERV-K in Merlin-negative schwannoma and meningioma tumours.

Key words: schwannoma, meningioma, NF2, HERV-K(HML2)

*Corresponding authors.

Email: sylwia.ammoun@plymouth.ac.uk . Faculty of Health: Medicine, Dentistry and Human Sciences, Plymouth University, John Bull Building, Plymouth Science Park, Research Way, Plymouth, PL6 8BU, UK. Phone: +441752 437419

Email: rbelshaw@kean.edu . College of Science and Technology, Wenzhou-Kean University, 88 Daxue Road, Ouhai, Wenzhou, Zhejiang Province, China 325060. Phone: +86 1985 881 7303

No potential conflicts of interest were disclosed

Word count: 4987

Total number of figures: 7

Supplementary figures: 7

Supplementary tables: 4

Abstract

1   Deficiency of the tumour suppressor Merlin causes development of schwannoma, meningioma,

2   and ependymoma tumours, which can occur spontaneously or in the hereditary disease

3   neurofibromatosis type 2 (NF2). Merlin mutations are also relevant in a variety of other

4   tumours. Surgery and radiotherapy are current first-line treatments; however, tumours

5   frequently recur with limited treatment options. Here, we use human Merlin-negative

6   schwannoma and meningioma primary cells to investigate the involvement of the endogenous

7   retrovirus HERV-K in tumour development. HERV-K proteins previously implicated in

8   tumorigenesis were overexpressed in schwannoma and all meningioma grades, and disease-

9   associated CRL4DCAF1 and YAP/TEAD pathways were implicated in this overexpression. In

10   normal Schwann cells, ectopic overexpression of HERV-K Env increased proliferation and

11   upregulated expression of c-Jun and pERK1/2, which are key components of known

12   tumorigenic pathways in schwannoma, JNK/c-Jun and RAS/RAF/MEK/ERK. Furthermore,

13   FDA-approved retroviral protease inhibitors ritonavir, atazanavir, and lopinavir reduced

14   proliferation of schwannoma and grade I meningioma cells. These results identify HERV-K as

15   a critical regulator of progression in Merlin-deficient tumours and offer potential strategies for

16   therapeutic   intervention.

17

18   Significance:

19   The endogenous retrovirus HERV-K activates oncogenic signalling pathways and promotes

20   proliferation of Merlin-deficient schwannomas and meningiomas, which can be targeted with

21   anti-retroviral drugs and TEAD inhibitors.

Introduction

Deficiency of the tumour suppressor Merlin leads to the development of multiple tumours of the nervous system such as schwannomas, meningiomas and ependymomas, which occur spontaneously or as part of the hereditary disease Neurofibromatosis type 2 (NF2) [1]. NF2 commences in childhood/early adolescence, and it is common that patients develop multiple tumours simultaneously. Current treatments for Merlin-deficient tumours are restricted to surgery or radiosurgery, which have limitations when tumours occur at multiple sites or are situated where resection would risk neurological complications. An international meeting of researchers, clinicians, pharmaceutical companies, and patient advocates has stressed the urgent need to accelerate clinical trials [1]. The fastest way towards clinical trials is drug-repurposing, an approach pursued by the NF2 research community [2].

In this study we investigate Merlin-deficient schwannomas and meningiomas, and a potential therapeutic target called Human Endogenous Retrovirus (HERV) type K lineage HML2 (HERV-K).

HERVs are the results of ancient germline retroviral infections that have been transmitted over the generations in a Mendelian fashion, and in total they comprise 8% of the human genome, with HERV-K consisting of approximately 100 individual viral sequences [3]. HERV-K proteins – Env, Rec and Np9 – are linked to tumourigenesis [4-8] and are upregulated in a variety of cancers [9]. Several FDA-approved HIV protease inhibitors appear to both affect HERV-K [10; 11] and show promise as anticancer drugs via other mechanisms [12], such as inhibition of Retinoblastoma (RB1) and phospho-AKT and downregulation of S phase genes [13].

We use an *in vitro* model for Merlin-deficient tumours consisting of patient-derived tumour cells that are cultured up to five passages. This model, in contrast to immortalised cell lines, more closely represents the *in vivo* tumour, thus facilitating the translation of *in vitro* studies

47 to phase 0 clinical trials [14-17]. We demonstrate that (i) HERV-K Env, Gag, Rec and Np9

48 proteins are overexpressed in human Merlin-negative schwannoma (Sch-NF2-/-) and in all

49 meningioma grades, (ii) ectopic Env overexpression in Schwann cells (Sch-NF2+/+)

50 upregulates mitogenic pERK and c-Jun protein levels and increases proliferation, (iii) HERV-

51 K Env is upregulated by Merlin-deficiency via the CRL4^{DCAF1} and YAP/TEAD pathway, (iv)

52 three FDA-approved antiretroviral drugs decrease both Sch-NF2-/- and Merlin-negative grade

53 I meningioma (MN-GI-NF2-/-) cell proliferation.

54 **Materials and Methods**

55 **Cell culture**

56 Schwannoma and meningioma tissues were from Derriford Hospital (Plymouth, UK) and

57 Southmead Hospital (Bristol, UK) under local R&D approval (Plymouth Hospitals NHS Trust:

58 R&D No. 14/P/056 and North Bristol NHS Trust: R&D No. 3458). Normal peroneal nerve

59 tissues (NNT) were from BRAIN UK (Neuropathology Department, Derriford Hospital),

60 normal Schwann cells (sural nerve) from post-mortem donors (Derriford Hospital), normal

61 meningeal tissues (NMT) from Novus Biologicals® and Analytical Biological Services Inc.,

62 and Human Meningeal Cells (HMC) from ScienCell Research Laboratories. All meningiomas

63 were graded by neuropathologist. Participants provided written informed consent and the study

64 was conducted in accordance with the Declaration of Helsinki under institutional review board

65 approval. Patient data are given in supplementary Tables 1 and 2. Schwannoma and Schwann

66 cells were cultured as previously described [14]. All schwannoma cells and tissues used in this

67 study are Merlin-negative and all Schwann cell cultures are S100 positive. Grade I meningioma

68 cells were cultured as previously described [18]. All experiments except for some IHC were

69 performed in Merlin-negative meningiomas. The human embryonic kidney (HEK) 293T cell

70 line was grown in DMEM supplemented with 10% FBS and 100U/ml penicillin/streptomycin

71 at 37ºC (5% CO_2).

Inhibitors

Ritonavir (Cat# SML0491), Atazanavir (Cat# SML1796), Lopinavir (Cat# SML1222), Sorafenib (Cat# SML2653), Selumetinib (Cat# AMBH2D6F1825) were from Sigma-Aldrich. Verteporfin (Cat# 5305) was from Tocris Bioscience, Bio-Techne and VT107 from Vivace Therapeutic.

Lentiviruses

CRL4^{DCAF1} shRNA and scramble shRNA lentiviruses were provided by J. Lyons-Rimmer (Plymouth University, Plymouth, UK) or purchased from Santa Cruz (Cat# sc-76898-V, Cat# sc-108080). A HERV-K Env-expressing lentiviral vector and the empty vector were a kind gift from M. Dewannieux (Gustave Roussy Institute, Villejuif, France) [7]. Lentiviral particles were produced by co-transfection of HEK 293T cells with the lentiviral vector, packaging plasmids (pCMV-DR8.2; pVSV-G) in combination with MegaTran 1.0 (Cat# TT200005, Origene) mixed in Opti-MEM™ (Cat# 31985062, Thermofisher Scientific). Cells were incubated with lentiviral particles and 16-20 µg/ml protamine sulphate (Cat# 107689, Sigma-Aldrich) for 72 hours followed by selection with either 63.2 μg/ml Hygromycin B (Cat# 10687010, Thermofisher scientific; Env overexpression) or 4.0 μg/mL puromycin (Cat# P9620, Sigma-Aldrich; CRL4^{DCAF1} knockdown).

Western Blotting

Western blotting (WB) was performed as previously described [19] using anti-HERV-K Env (Cat# HERM-1811-5, AMSBIO), anti-HERV-K Gag (Cat# HERM-1841-5, AMSBIO), anti-phospho ERK (Cat# V803A, Promega), anti-ERK (Cat# 4695, New England Biolabs), anti-CRL4^{DCAF1} (Cat# 11612-1-AP, Proteintech), anti-CTGF (Cat# ab6992, Abcam), anti-YAP (Cat# 14074, New England Biolabs), anti-Pan TEAD (Cat# 13295, New England Biolabs), anti-CD63 (Cat# 10628D, Thermofisher Scientific) and anti-Merlin (Cat# 6995, New England Biolabs) antibodies. For detection, secondary HRP-conjugated antibodies (Cat# 170-6516 and

97   Cat# 172-1019, Biorad) and Pierce ECL or Pierce ECL Plus substrates (Cat# 32209, Cat#

98   32132X3, Thermofisher Scientific) were used. Anti-GAPDH (Cat# MAB374, Merck

99   Millipore) and anti-Tubulin α (ab4074, Abcam) antibodies were used for loading controls. WB

100 bands densities were quantified using ImageJ software.

Immunocytochemistry

102 Immunocytochemistry (ICC) was performed as previously described [19] using anti-Rec and

103 anti-Np9 polyclonal sera (kindly provided by F. Grässer, Universitätsklinikum des Saarlandes,

104 Homburg, Germany) and anti-HERV-K Env (Cat# HERM-1811-5, AMSBIO), anti-HERV-K

105 Gag (Cat# HERM-1841-5, AMSBIO), anti-CD63 (Cat#10628D, Thermofisher Scientific),

106 anti-CD9 (Cat# orb235075, Biorbyt) and anti-c-Jun (Cat# 9165, New England Biolabs)

107 antibodies.

108 Proliferating or apoptotic cells were detected using anti-Ki67 (Cat# M7420, Agilent) and anti-

109 Cleaved Caspase 3 Asp 175 (Cat# 9661, Cell Signaling Technology) antibodies respectively.

110 Secondary goat-anti-mouse Alexafluor 488 or 594 (Cat# A11001, Cat# A11005, Thermofisher

111 Scientific) and goat-anti-rabbit Alexafluor 488 or 568 (Cat# A11008, Cat# A11011,

112 Thermofisher Scientific) were used for detection. DAPI (Cat# D9542, Thermofisher Scientific)

113 counter-stained nuclei were used for visualisation.

Immunohistochemistry

115 The 5-μm paraffin-embedded tissue sections were deparaffinized, pre-treated in Tris/EDTA

116 buffer (2.4mg/ml Tris, 0.2mg/ml EDTA, 2mM HCl pH9.0) for anti-HERV-K Gag and in citrate

117 buffer (2.1mg/ml citric acid, 10mM NaOH, pH6.0) for anti-HERV-K Env, and heated for 30

118 minutes. Tissue preparations were then incubated overnight with the primary antibodies (1:50).

119 VECTASTAIN Elite ABC HRP Kit Universal (Cat# PK-6200, Vector Laboratories) was used

120 for detection.

121

Merlin re-introduction

Merlin wild type (NF2-Ad) and control GFP (GFP-Ad)-containing adenovirus vectors were a kind gift from J. Testa (Fox Chase Cancer Center, Philadelphia, PA). Cells were infected for 24 hours followed by incubation in fresh culture medium for an additional 48 hours. Successful infection was determined by the presence of GFP, and Merlin expression was quantified by WB.

De-glycosylation of cellular proteins

Cell lysates were treated with 5% sodium dodecyl sulphate, 1M Dithiothreitol, 0.5M sodium phosphate buffer (pH7.5), 10% Triton X-100 and PNGase F (Cat# V4831, Promega) at 37ºC for 1-3 hours.

Exosome isolation

Cells were cultured for seven days in medium containing exosome-depleted FBS (Cat# EXO-FBS-250A-1, System Biosciences). Exosomes were isolated using Total Exosome Isolation Reagent (Cat# 4478359, Thermofisher Scientific). Exosomes were lysed with RIPA buffer supplemented with protease and phosphatase inhibitors [18]. HERV-K Env and CD63 (exosome marker [20]) levels were assessed by WB. Tubulin was used as a cytoplasmic marker and Colloidal Gold Total Protein Stain (Cat#1706527, Biorad) was used as a loading control.

TEAD binding site

TEAD binding motifs (TGGAAT) were searched within HERV-K promoter regions using an alignment of proviruses [3] followed by chromatin immunoprecipitation sequencing (ChIP-Seq) (CD Genomics, USA).

Microscopy

Images were acquired with Zeiss LSM510 (Zeiss, Oberkochen, Germany) and Leica SPE (Leica Microsystems, Wetzlar, Germany) confocal units attached to Zeiss Axiovert and Leica IM8 microscopes respectively. Co-localisation was performed using z-stack. Proliferation assays used a 20x air objective and all other experiments were imaged using a 40x oil pH2 objective. Zeiss image manipulation software (ZEN) was used for editing.

Data Analysis

Except for the IHC data, unpaired Student's two-tailed t-tests and one-way ANOVA with post-hoc Tukey statistical tests were used. Experiments were performed using samples from at least three different individuals. Mann-Whitney U tests were used on IHC data (GraphPad Prism). Scoring of IHC staining was done blind and was as follows: 0 = negative, 1 = weakly positive, 2 = moderately positive, 3 = strongly positive. Statistical values are as follows: ns (not significant) $p > 0.05$, * $p < 0.05$, ** $p < 0.01$, *** $p < 0.001$. In figures the mean $\pm$ SEM is given.

158 **Results**

159 **HERV-K proteins are overexpressed in Merlin-negative schwannoma**

160 Firstly, we determined HERV-K protein expression in human schwannoma tissues and primary

161 cells, as well as control Schwann cell, by immunohistochemistry (IHC), immunocytochemistry

162 (ICC) and western blotting (WB). In IHC nine of 10 Merlin-negative schwannoma (Sch-NF2-

163 /-) tissues and four of 10 Merlin-positive (NF2+/+) normal nerve tissues stained positively for

164 HERV-K Env, with the staining intensity in schwannomas usually higher (Mann-Whitney U

165 test, P=0.009) (Fig. 1A). Correspondingly, ICC revealed strong HERV-K Env staining (in the

166 cytoplasm and at the cell membrane) in both permeabilised and non-permeabilised Sch-NF2-

167 /- cells *in vitro*, but staining was negligible in normal Schwann cells (Sch-NF2+/+) (Fig. 1B).

168 Increased nuclear staining of HERV-K Rec and Np9 was also observed in Sch-NF2-/-

169 compared to Sch-NF2+/+ cells (Fig. 1C).

170 The upregulation of HERV-K Env was verified by WB. HERV-K Env is translated as a full-

171 length Env (Env-FL) precursor that is cleaved into a surface unit (Env-SU) and a

172 transmembrane unit (Env-TM), and the anti-HERV-K Env antibody used binds to the latter.

173 WB in Sch-NF2+/+ cells after ectopic overexpression of Env (Fig. S1A) confirmed the

174 presence of both Env-FL and Env-TM proteins at the expected sizes of ~98 kDa and ~36 kDa

175 respectively [21]. We also confirmed that Env-FL is glycosylated by using Peptide N-

176 glycosidase (PNGase) treatment in Sch-NF2-/- cells (Fig. S1B) [21]. WB in Sch-NF2-/- tissues

177 demonstrated significant upregulation of both Env-TM and Env-FL (Fig. 1D-F), as well as Rec

178 and Np9 (Fig. 1D, G, H) proteins in Sch-NF2-/- tissues compared to very weak expression in

179 normal nerve tissues (NNT). WB in Sch-NF2-/- cultured cells confirmed the above, revealing

180 significant Env-FL and Env-TM upregulation in tumour cells compared to normal Sch-NF2+/+

181 cells (Fig. 1I, J).

182   Merlin re-introduction into Sch-NF2-/- cells using a Merlin-expressing adenovirus (NF2-Ad)

183   significantly reduced the expression of HERV-K Env-FL by ~30% and Env-TM by ~60% (Fig.

184   1K, L).

185   In addition to the potentially tumourigenic proteins – Env, Rec and Np9 – we confirmed that

186   HERV-K is upregulated in Sch-NF2-/- cells and tissues using another HERV-K protein,

187   namely Gag. IHC demonstrated moderate or strong expression of HERV-K Gag in 13 of 15

188   Sch-NF2-/- tissues compared to only three of 15 NNT (Mann-Whitney U test, P=0.0002; Fig.

189   S1D), which was confirmed by ICC in primary Sch-NF2-/- cells (Fig. S1E). WB also

190   demonstrated significant HERVK-Gag-FL overexpression in Sch-NF2-/- cells (the increase in

191   mean HERVK-p15+CA/CA+NC expression was not significant) (Fig. S1F, G).

192   **HERV-K Env protein contributes to schwannoma development**

193   We selected c-Jun and pERK as mitogenic/tumourigenic markers in schwannoma.

194   Transcription factor c-Jun is a master regulator of Schwann cells (Sch-NF2+/+) differentiation

195   and its expression strongly increases following nerve injury, which results in reactivation of

196   proliferation [22]. C-Jun and its upstream activator, phosphorylated c-Jun N-terminal kinase

197   (pJNK), are highly expressed in Merlin-negative schwannoma (Sch-NF2-/-) cells compared to

198   normal Merlin-positive (Sch-NF2+/+) cells and contribute to increased cell proliferation and

199   survival [23, 24]. pERK is also strongly activated in Sch-NF2-/- cells and, in addition to pJNK,

200   is a component of the key mitogenic pathway [15; 17].

201   We demonstrate that ectopic overexpression (o/e) of Env in Sch-NF2+/+ cells (Fig. 2A) did

202   indeed increase proliferation (percentage of total cells monitored by DAPI that were Ki67+;

203   (Fig. 2B, C), upregulated c-Jun expression (Fig. 2D, E) and increased levels of active pERK

204   (Fig. 2F, G).

205   The involvement of HERV-K Env in Sch-NF2-/- cell proliferation is further supported by our

206   observation that the monoclonal anti-HERV-K Env antibody added to cell culture medium

207 significantly reduced proliferation (Fig. 2H, J) and decreased the activity of pERK (Fig. 2L,

208 M) in Sch-NF2-/- cells. Importantly, no effect of the antibody on normal Sch-NF2+/+ cells

209 proliferation was observed (Fig. 2I, K).

HERV-K Env protein is released via exosomes in Merlin-negative schwannoma

211 The observation that the anti-HERV-K Env antibody reduced proliferation in Merlin-negative

212 schwannoma (Sch-NF2-/-) cells suggested that HERV-K Env action may also involve

213 autocrine or paracrine signalling. Retroviral Env proteins are responsible for attachment of the

214 viral particle to host cells, and the physiologically important Env proteins of another HERV

215 family, Syncytin-1 and Syncytin-2, are crucial for exosome binding and internalization [25].

216 We therefore investigated whether HERV-K Env is present in Sch-NF2-/- exosomes. ICC and

217 confocal microscopy showed some HERV-K Env co-localisation in the cytoplasm with the late

218 endosome/exosome marker CD9 (Fig. 3A). WB of exosomes extracted from Sch-NF2-/- cell

219 culture medium collected after seven days of culture, using the additional late

220 endosome/exosome marker CD63, revealed that the HERV-K Env protein is released from

221 Sch-NF2-/- cells via exosomes and that the release is significantly increased in Sch-NF2-/-

222 cells compared to Sch-NF2+/+ cells (Fig. 3B, C). Note, the levels of Env-FL could not be

223 measured due to a co-migrating band seen in negative control samples (which is the exosome

224 fraction from culture medium not exposed to cells) (Fig. S1C). No Env protein was detected in

225 exosome-free supernatant fractions collected after exosome isolation (Fig. 3B).

Mechanism of HERV-K upregulation downstream of Merlin

227 To understand why HERV-K is overexpressed in Merlin-deficient tumours we first

228 investigated NFκB, which is strongly overexpressed in Merlin-negative schwannoma (Sch-

229 NF2-/-) cells due to Merlin-deficiency and activates mitogenic signalling pathways [17]. NFκB

230 is known to bind to and stimulate HERV-K expression [26]. However, by using the NFκB

231 inhibitor SN50 at a concentration that inhibits NFκB translocation into the nucleus and

232 activation, and target gene expression [7] (Fig. S2A-D) – we demonstrated that NFκB is not

233 involved in HERV-K expression in Sch-NF2-/- cells.

234 Next, we investigated if the CRL4^{DCAF1} and YAP/TEAD pathways, both of which are activated

235 in Merlin-deficient tumours [27], are involved in the increased expression of HERV-K.

236 Depletion of CRL4^{DCAF1} by shRNA knockdown significantly decreased Env-FL expression

237 (Fig. 4A, B, K; by ~20-30% with one construct and by ~50-60% with a second construct).

238 Inhibition of the downstream YAP/TEAD interaction, which prevents TEAD-mediated

239 transcription, using either the YAP inhibitor Verteporfin (which promotes 14-3-3σ/YAP

240 sequestration in the cytoplasm and its subsequent degradation [28]) or a novel TEAD-specific

241 inhibitor VT107 (Vivace Therapeutics) [29] decreased expression of the HERV-K Env proteins

242 by ~40-50% (Fig. 4C, D, I-K). The efficacy of the drugs was demonstrated by decreased

243 expression of CTGF (a target gene of YAP/TEAD transactivation), YAP and Pan-TEAD (Fig.

244 4C, I, J). In addition, Verteporfin decreased proliferation (Ki67) in Sch-NF2-/- cells (Fig. 4E,

245 F) but had no effect on the proliferation of normal Schwann cells (Sch-NF2+/+) (Fig. 4G, H).

246 Further downstream involvement of this pathway was suggested by the presence of a TEAD

247 binding site on the HERV-K sequence *in silico* (Fig. S3); however, ChIP-Seq detected only a

248 12% increase in the number of HERV-K matches compared to the experimental control.

249 Thus, HERV-K upregulation is at least in part triggered by CRL4^{DCAF1} and YAP/TEAD Hippo

250 pathway deregulation due to Merlin-deficiency.

251 **Repurposing antiretroviral drugs in Merlin-negative schwannomas**

252 We tested whether three FDA-approved retroviral protease inhibitors – Ritonavir, Atazanavir

253 and Lopinavir – have an anti-proliferative effect on Merlin-negative schwannoma (Sch-NF2-

254 /-) cells. All have been reported to have affinity for HERV-K protease [10; 11].

255 Ritonavir decreased Sch-NF2-/- cells proliferation (Ki67) with a half maximal inhibitory

256 concentration (IC50) of 2.9 μM (Fig. 5A, C, and Table S3). This is 7.6-fold lower than the peak

plasma concentration (Cmax) of 22 µM, and 3.6-fold lower than the trough plasma concentration (Cmin) of 10.4 µM observed in HIV patients without side-effects [30]. Importantly, Ritonavir had no effect on normal Schwann cells (Sch-NF2+/+) proliferation (Fig. 5B, C). In addition, Ritonavir significantly downregulated two major proliferation markers in schwannoma: pERK, with IC50=1.35 µM, and cyclin D1 [17], with IC50=2.31 µM (Fig. 5D, S4A, and Table S3). As expected, Ritonavir appears to inhibit the HERV-K protease in Sch-NF2-/- cells, causing an increased expression of the uncleaved Gag-FL precursor protein and decreased expression of the second main band, which we interpret as representing cleaved p15+CA (15 kDa protein + capsid) and/or cleaved CA+NC (capsid + nucleocapsid) proteins (our antibody binds to CA) with IC50=1.31 µM (Fig. 5D, S4B, and Table S3) [31]. In contrast to Gag, the Env-FL precursor protein is cleaved by a human furin proteases rather than the retroviral protease [32] and Ritonavir treatment decreased the expression of both Env-FL (IC50= 1.23 µM) and Env-TM (IC50=0.55 µM) (Fig. 5D, Fig. S4C, and Table S3).

Lopinavir was as effective as Ritonavir and decreased Sch-NF2-/- cells proliferation with IC50=3.66 µM, which is ~4.7-fold lower than the plasma Cmax (~17 µM) and ~2.6-fold lower than Cmin (~9.4 µM) assessed by a pharmacokinetics study [33] (Fig. 5E, G, and Table S3). In addition to inhibiting cell proliferation, Lopinavir decreased pERK with IC50= 1.26 µM (Fig. 5H, S4D, and Table S3), inhibited Gag-FL cleavage and decreased cleaved p15+CA and/or CA+NC with IC50=1.38 µM [10] and decreased the levels of Env-TM (IC50=8.78×10^{-3} µM) (Fig. 5H, S4E, F and Table S3). Atazanavir appears to be less effective than Ritonavir and Lopinavir. This drug decreased Sch-NF2-/- cell proliferation with IC50=7.38 µM, which is ~1.8-fold higher than the Cmax (~4.1 µM) and ~10-fold higher than Cmin (~0.7 µM) [33] (Fig. 5F, G, and Table S3).

Ritonavir has an additive effect with Selumetinib and Sorafenib *in vitro*

Ritonavir, in addition to its antiretroviral proprieties, can also inhibit CYP3A4 and thereby boost efficacy of drugs which are metabolised by CYP3A4 [34]. We therefore investigated whether Ritonavir would increase efficacy of the MEK inhibitor Selumetinib and the PDGFR/Raf inhibitor Sorafenib, both of which reduce proliferation of Merlin-negative schwannoma (Sch-NF2-/-) cells *in vitro* [15] and are known CYP3A4 substrates [35; 36]. Sorafenib has been tested in phase 0 clinical trials in NF2 patients [37]. Treating Sch-NF2-/- cells with Ritonavir in combination with Selumetinib or Sorafenib showed that both Ritonavir+Sorafenib and Ritonavir+Selumetinib combinations have additive effects (Fig. 5I-K).

HERV-K plays a similar role in Merlin-negative meningioma

An increase of HERV-K expression was demonstrated by WB in all grades of Merlin-negative meningioma tissues (grade I, MN-GI-NF2-/-; grade II, MN-GII-NF2-/-; grade III, MN-GIII-NF2-/-) and in MN-GI-NF2-/- primary cells compared to control normal meningeal tissues (NMT) and Human Meningeal Cells (HMC), respectively.

Env-FL and Np9 expression in MN-GI-NF2-/- and MN-GII/III-NF2-/- tissues were increased (Env-FL average ~7-fold for G-I and average ~10-fold for GII/III; Np9 average ~4-fold for G-I and average ~12-fold for G-II/III) although not significantly compared to NMT (Fig. 6A, C, D, G). Env-TM was significantly increased in MN-GI-NF2-/- tissues (average ~7-fold) but not in MN-GII/III-NF2-/- tissues (Fig. 6A, E). Rec was observed only in MN-GI-NF2-/- and MN-GII/III-NF2-/- biopsies, but not in NMT (Fig. 6B, F). Gag-FL expression was higher in MN-GI-NF2-/- and MN-GII/III-NF2-/- biopsies although not significantly (Fig. S5A, B). Gag products p15+CA/CA+NC were significantly increased in MN-GI-NF2-/- but not in MN-GII/III-NF2-/- biopsies compared to NMT- (Fig. S5A, C).

306 The expression of Env-FL (Fig. 6H, I) and Gag-FL (Fig. S5D, E) was significantly increased

307 in MN-GI-NF2-/- primary cells (Env-FL average ~3-fold; Gag-FL average ~6-fold) compared

308 to HMC. The difference in the expression of Env-TM (Fig. 6H, I), and p15+CA/CA+NC (Fig.

309 S5D, F) was however not significant.

310 IHC demonstrated moderate or strong staining for HERV-K Env in all eight MN-GI-NF2-/-

311 tumours (Fig. S5G, I). Eight of 10 control NMT tissues were also positive for HERV-K Env

312 but the average staining intensity was significantly weaker (Fig. S5G, I; Mann-Whitney U test,

313 P=0.0015). HERV-K Gag staining was also moderate or strong in all eight MN-GI-NF2-/-

314 tissues and the average staining intensity was significantly higher compared to NMT (Fig. S5H,

315 J; Mann-Whitney U test, P=0.0005). We observed similar results with the higher meningioma

316 grades for HERV-K Env (Fig. S5G, I; Mann-Whitney U test, P=0.0015 grade II, and P<0.0001

317 grade III) but not for HERV-K Gag (Fig. S5H, J; Mann-Whitney U test, P= 0.6667 for grade

318 II, and P= 0.0561 for grade III). However, the Merlin status of some of these tissues used in

319 IHC was not recorded (not determined ND) (Fig. S5G-J).

320 The specificity of the anti-HERV-K Env antibody in control HMC cells was confirmed by

321 ectopic overexpression of Env (Fig. S5K). Env overexpression in MN-GI-NF2-/- cells was also

322 reversed by Merlin re-introduction (Fig. 6J, K) and significantly decreased by the TEAD-

323 specific inhibitor VT107 (Fig. 6L, M), confirming the involvement of CRL4^{DCAF1} and

324 YAP/TEAD Hippo pathway in the regulation of HERV-K overexpression in meningioma.

325 Although, some intracellular co-localisation of Env with late endosome/exosome marker CD63

326 was observed (Fig. S5L), no exosome-mediated Env release was detected in either HMC or

327 MN-GI-NF2-/- cells (Fig. S5M).

328 **Repurposing antiretroviral drugs in Merlin-negative meningiomas**

329 Ritonavir, Atazanavir and Lopinavir all strongly decreased proliferation (Ki67) of Merlin-

330 negative grade I meningioma (MN-GI-NF2-/-) cells displaying even stronger inhibition than in

331 Sch-NF2-/- cells (Fig. 7A-D, Table S4). Ritonavir decreased the number of proliferating cells

332 with IC50=0.61 µM (~36-fold lower than plasma Cmax and ~17-fold lower than plasma Cmin

333 in HIV patients [30]) (Fig. 7A, D, and Table S4), Atazanavir with IC50=0.14 µM (~29-fold

334 lower than plasma Cmax and ~5.2-lower than plasma Cmin [33]) (Fig. 7B, D, and Table S4)

335 and Lopinavir with IC50=0.88 µM (~19-fold lower than plasma Cmax and ~9-fold lower than

336 plasma Cmin [33]) (Fig. 7C, D, and Table S4). Cell viability was not affected at drug

337 concentrations 1 µM, 5 µM and 10 µM (Fig. S6 A). However, at Cmax concentrations,

338 Ritonavir (22 µM [30]) and Lopinavir (17 µM [33]) induced death of almost 100% of tumour

339 cells (Fig. S6 B). Atazanavir at its Cmax concentration (4.1 µM) [33] was not toxic.

340 In addition, Ritonavir, Atazanavir and Lopinavir all significantly decreased active pERK

341 (Ritonavir, IC50=8.73 µM; Atazanavir, IC50 was not calculable, and Lopinavir IC50=4.07

342 µM) and cyclin D1 (Ritonavir, IC50=4.41 µM; Atazanavir, IC50=6.3 µM, and Lopinavir

343 IC50=3.05 µM) (Fig. 7E, Fig. S7, and Table S4). They also inhibited the retroviral protease,

344 causing increased expression of Gag-FL and decreased expression of p15+CA/CA+NC

345 (Ritonavir, IC50=186.82 µM, ~35% decrease at 10 µM; Atazanavir, IC50=12.51 µM, and

346 Lopinavir, IC50=6.19 µM) (Fig. 7E, Fig. S7, and Table S4). All three drugs reduced the

347 expression of both Env-FL and Env-TM (Ritonavir, Env-FL IC50=57.22 µM, ~40% decrease

348 at 1µM; Env-TM IC50=1.13×10^3µM, ~30% decrease at 10 µM), Atazanavir (Env-FL,

349 IC50=2.95 µM; Env-TM IC50=2.3×10^3µM, ~35% decrease at 1µM), and Lopinavir (Env-FL

350 IC50=0.89 µM, Env-TM IC50=0.54 µM) (Fig. 7E, Fig. S7, and Table S4).

Discussion

Potential therapeutics for schwannomas and meningiomas

This report suggests the use of antiretroviral protease inhibitors to treat patients with Merlin-deficient schwannomas and meningiomas. In both Merlin-negative schwannoma (Sch-NF2-/-) cells and Merlin-negative meningioma (MN-GI-NF2-/-) cells, Ritonavir and Lopinavir (and, for meningioma, Atazanavir) decreased proliferation, with an IC50 lower than the Cmin in HIV patients. In addition, Ritonavir had no effect on proliferation of normal Merlin-positive Schwann (Sch-NF2+/+) cells, suggesting that it is tumour selective (we lacked sufficient samples to test Lopinavir and Atazanavir). Interestingly, the effect of all three drugs was much stronger against meningiomas.

The pleiotropic anticancer effects of antiretroviral drugs (not just protease inhibitors) have attracted interest recently [38]. For example, there have been at least 20 clinical trials involving Ritonavir in a broad range of cancer therapies, three of which also involved Lopinavir. Most trials have not yet reported but a Ritonavir plus Lopinavir phase II trial in high-grade gliomas found that the drugs were well tolerated but did not significantly improve six-month progression-free survival among 19 patients [39]. In antiretroviral therapy, Ritonavir is now used primarily in combination with Atazanavir or Lopinavir to boost the latter's bioavailability, *e.g.* by its CYP3A4-inhibitory properties mentioned above [34]. We found Ritonavir to have an additive effect in combination with Sorafenib or Selumetinib.

Treatment of tumours such as schwannomas and meningiomas, especially when occurring as part of the NF2 disease, must be for prolonged periods of time which risks the development of long-term adverse effects. The low IC50 observed in treatment of Sch-NF2-/-cells and MN-GI-NF2-/- cells *in vitro* suggests one could use a low dose in the medication regimen. Also, both schwannoma and meningioma tumours are located outside the blood-brain barrier and thus drug delivery should not be problematic. Our recent phase 0 clinical trial of orally

376 administered Sorafenib in NF2 patients achieved high intratumoural concentration of the drug

377 [37].

378 Another possible treatment is immunotherapy with a humanised anti-HERV-K Env antibody

379 [40]. Although HERV-K Env is upregulated in Sch-NF2-/- and MN-GI-NF2-/- cells and

380 tissues, it is expressed at lower levels in normal Sch-NF2+/+ cells and meningeal cells. An

381 immunotherapy approach would therefore need careful safety testing.

382 Further testing with a mouse model is impossible. There is an NF2 mouse model [41], but

383 HERV-K occurs only in humans [3; 9]. Implantation of human schwannoma into mice

384 vestibular nerves is surgically impossible, and sub-cutaneous xenograft would not recapitulate

385 the unique intraneural microenvironment for schwannoma growth.

386 *Mechanism of retroviral protease inhibitors*

387 The mechanism at play in the antiretroviral drug-driven proliferation inhibition is probably

388 multifaceted and involving both HERV-K-dependent and -independent pathways. For

389 example, in addition to having an inhibitory effect on HERV-K protease, Ritonavir is known

390 to inhibit proteasome activity, although only at higher concentrations (>10μM) [42]. In a study

391 using human glioblastoma-derived cells GL15, Ritonavir inhibited chymotrypsin-like activity

392 of the proteasome with IC50=50μM and significantly induced cell cycle arrest at concentration

393 of 100 μM [42]. In our study, however, Ritonavir decreased proliferation of Merlin-negative

394 schwannoma (Sch-NF2-/-) and Merlin-negative grade I meningioma (MN-GI-NF2-/-) cells at

395 IC50=2.9 μM and IC50=0.61 μM respectively. These concentrations are much lower than

396 needed for effective proteasome inhibition and perhaps indicate that Ritonavir's proteasome

397 inhibitory effect is a minimal contribution to the inhibition of HERV-K levels.

398 Moreover, both Ritonavir and Lopinavir inhibited pERK activity, which we think may be partly

399 due to overexpression of HERV-K. We confirmed the effect of both drugs on the HERV-K

400 protease, which cleaves the viral Gag protein. Less expectedly, the drugs also inhibited the

401   expression of HERV-K Env, which is cleaved by a cellular furin-like endoprotease [32]. Since

402   levels of both the uncleaved Env-FL precursor and cleaved Env-TM were decreased, the drugs

403   did not affect the cleavage efficiency as with Gag but rather the overall expression of HERV-

404   K Env. This is perhaps consistent with these drugs having a broad range of effects.

405   *HERV-K upregulation (Transcription factors)*

406   We demonstrated that HERV-K Env expression is dependent on the tumour suppressor Merlin.

407   There is evidence of another HERV, HERV-E, being upregulated by inactivation of another

408   tumour suppressor: von Hippel–Lindau (VHL) protein [43]. Downstream of Merlin, we

409   suggest for the first time that HERV-K Env expression in both Merlin-negative schwannoma

410   (Sch-NF2-/-) cells and Merlin-negative grade I meningioma (MN-GI-NF2-/-) is regulated by

411   the transcription factor TEAD via binding to YAP. We observed that TEAD possesses a

412   binding domain on HERV-K Long Terminal Repeats (LTR) *in silico.* However, we were

413   unable to confirm binding with our ChIP analysis. This failure to confirm binding might be

414   caused by the approximately 1,000 fragments of HERV-K scattered across the genome [3].

415   Blocking different elements in the Hippo pathway, as well as CRL4^{DCAF1}, reduced but did not

416   completely block HERV-K expression, suggesting the involvement of additional factors. One

417   such factor could be Src, which activates YAP [44] and has been previously shown by us to be

418   involved in increased Sch-NF2-/- cell proliferation downstream of PDGFRβ [14] and integrin

419   β1 [45]. Other possible factors are that HERV-K loci are often silenced by methylation and

420   have binding sites for many transcription factors, at least eight of which have been

421   demonstrated experimentally to upregulate HERV-K [46] (although our study allows us to

422   exclude one, NFκB, in schwannomas).

423   *HERV-K Env signalling pathways*

424   HERV-K Env has been previously demonstrated to contribute to tumourigenesis of melanoma,

425   breast and pancreatic cancers involving MYC, AKT and – especially – RAS/RAF/MEK/ERK

426 signalling pathways [4-7]**.** We demonstrate that ectopic HERV-K Env overexpression in

427 normal Schwann cells induces proliferation and is associated with an upregulation of

428 phosphorylated/active ERK1/2 (pERK1/2), which is similar to that observed in schwannoma

429 tumour counterparts. In 293T cells, Env overexpression was also associated with pERK

430 upregulation involving the RAS/RAF/MEK/ERK pathway, a process requiring the presence

431 of Env cytoplasmic tail [7]. Which effector allows signal transduction from HERV-K Env to

432 RAF is unknown. The cytoplasmic tail of the Jaagsiekte sheep retrovirus (JSRV) Env, another

433 betaretrovirus envelope glycoprotein, harbours binding motifs for phosphatidylinositol 3-

434 kinase (PI3K), which is involved in the PI3K/AKT pathway leading to fibroblast

435 transformation [47]. However, the Lemaitre *et al.* study cited above [7] did not find

436 upregulation of pAKT.

437 Furthermore, we observed an increase in c-Jun suggesting that Env may also stimulate the

438 JNK/c-Jun network. C-Jun triggers proliferation of Schwann cells after nerve injury and is

439 overexpressed in schwannoma [22-24]**.** The phosphorylation profile in Env-knockdown cell

440 lines reveal downregulation of several kinases including c-Jun and JNK1/2/3 [6]**.** Therefore,

441 our findings are consistent with HERV-K Env contributing to schwannoma tumourigenesis by

442 the stimulation of the RAS/RAF/MEK/ERK and JNK/c-Jun pathways leading to increased cell

443 proliferation. We also found increased expression of Rec and Np9 proteins in schwannoma,

444 both of which are linked to tumour growth in other cancer types by altering pERK, Myc and

445 β-catenin pathways [48]**.** We have previously shown these pathways to be involved in

446 schwannoma development [16]**.**

447 We attempted HERV-K knockdown this using a large set of shRNAs targeting sites across the

448 provirus (LTR, *gag* and *env*). Our set included sequences that reduce Env expression in

449 pancreatic [6] and melanoma cell lines [5]. The shRNA used in pancreatic cells reduced growth

450   of cell lines inoculated in mice and reduced pERK expression as well as pAKT, MYC and

451   RAS. However, we were unsuccessful.

452   *HERV-K Env transport via exosomes*

453   HERV-K Env was detected at the cell membrane and in the exosomal fraction of culture

454   medium from schwannoma cells. We speculate that HERV-K Env, which is expressed on the

455   cell surface and has fusogenic ability [49], contributes to cell-to-cell transfer of growth factors

456   via exosomes. Thus, HERV-K Env would facilitate uptake of exosomes that are transporting

457   pro-tumoural molecules. Evidence for the pro-tumourigenic role of exosomes is accumulating

458   [50], and exosomal release of Env proteins (syncytins) from another HERV lineage (HERV-

459   W) has been reported to significantly increase the uptake of exosomes via receptor-facilitated

460   endocytosis [25]. Our observed anti-proliferative effect of the anti-HERV-K Env monoclonal

461   antibody might result from blocking this process.

462

References

464   1.   Blakeley JO, Evans DG, Adler J, Brackmann D, Chen R, Ferner RE, et al. Consensus
465   recommendations for current treatments and accelerating clinical trials for patients with
466   neurofibromatosis type 2. Am J Med Genet A. 2012;158A:24-41.
467   DOI:10.1002/ajmg.a.34359

468   2.   Chang LS, Oblinger JL, Smith AE, Ferrer M, Angus SP, Hawley E, et al. Brigatinib causes
469   tumor shrinkage in both NF2-deficient meningioma and schwannoma through inhibition of
470   multiple tyrosine kinases but not ALK. PLoS One. 2021;16:e0252048. DOI:
471   10.1371/journal.pone.0252048

472   3.   Subramanian RP, Wildschutte JH, Russo C, Coffin JM. Identification, characterization, and
473   comparative genomic distribution of the HERV-K (HML-2) group of human endogenous
474   retroviruses. Retrovirology. 2011;8:90. DOI:10.1186/1742-4690-8-90

475   4.   Oricchio E, Sciamanna I, Beraldi R, Tolstonog GV, Schumann GG, Spadafora C. Distinct
476   roles for LINE-1 and HERV-K retroelements in cell proliferation, differentiation and tumor
477   progression. Oncogene. 2007;26:4226-33. DOI:10.1038/sj.onc.1210214

478   5.   Zhou F, Li M, Wei Y, Lin K, Lu Y, Shenet J, et al. Activation of HERV-K Env protein is
479   essential for tumorigenesis and metastasis of breast cancer cells. Oncotarget.
480   2016;7:84093-117. doi:10.18632/oncotarget.11455

481   6.   Li M, Radvanyi L, Yin B, Rycaj K, Li J, Chivukula R, et al. Downregulation of Human
482   Endogenous Retrovirus Type K (HERV-K) Viral env RNA in Pancreatic Cancer Cells
483   Decreases Cell Proliferation and Tumor Growth. Clin Cancer Res. 2017;23:5892-911.
484   DOI:10.1158/1078-0432.CCR-17-0001

485   7.   Lemaître C, Tsang J, Bireau C, Heidmann T, Dewannieux M. A human endogenous
486   retrovirus-derived gene that can contribute to oncogenesis by activating the ERK pathway
487   and inducing migration and invasion. PLoS Pathog. 2017;13:e1006451.
488   DOI:10.1371/journal.ppat.1006451

489   8.   Denne M, Sauter M, Armbruester V, Licht JD, Roemer K, Mueller-Lantzsch N. Physical
490   and functional interactions of human endogenous retrovirus proteins Np9 and rec with the
491   promyelocytic leukemia zinc finger protein. J Virol. 2007;81:5607-16.
492   DOI:10.1128/JVI.02771-06

493   9.   Downey RF, Sullivan FJ, Wang-Johanning F, Ambs S, Giles FJ, Glynn SA. Human
494   endogenous retrovirus K and cancer: Innocent bystander or tumorigenic accomplice? Int J
495   Cancer. 2015;137:1249-57. DOI:10.1002/ijc.29003

496   10. Tyagi R, Li W, Parades D, Bianchet MA, Nath A. Inhibition of human endogenous
497   retrovirus-K by antiretroviral drugs. Retrovirology. 2017;14:21. DOI:10.1186/s12977-017-
498   0347-4

499   11. Kuhelj R, Rizzo CJ, Chang CH, Jadhav PK, Towler EM, Korant BD. Inhibition of human
500   endogenous retrovirus-K10 protease in cell-free and cell-based assays. J Biol Chem.
501   2001;276:16674-82. DOI:10.1074/jbc.M008763200

502   12. Maksimovic-Ivanic D, Fagone P, McCubrey J, Bendtzen K, Mijatovic S, Nicoletti F. HIV-
503   protease inhibitors for the treatment of cancer: Repositioning HIV protease inhibitors while
504   developing more potent NO-hybridized derivatives?. Int J Cancer. 2017;140:1713-26.
505   DOI:10.1002/ijc.30529

506   13. Batchu RB, Gruzdyn OV, Bryant CS, Qazi AM, Kumar S, Chamala S, et al. Ritonavir-
507   Mediated Induction of Apoptosis in Pancreatic Cancer Occurs via the RB/E2F-1 and AKT
508   Pathways. Pharmaceuticals (Basel). 2014;7:46-57. doi:10.3390/ph7010046

509   14. Rosenbaum C, Kluwe L, Mautner VF, Friedrich RE, Müller HW, Hanemann CO. Isolation
510   and characterization of Schwann cells from neurofibromatosis type 2 patients. Neurobiol
511   Dis. 1998;5:55-64. DOI:10.1006/nbdi.1998.0179

512   15. Ammoun S, Flaiz C, Ristic N, Schuldt J, Hanemann CO. Dissecting and targeting the
513   growth factor-dependent and growth factor-independent extracellular signal-regulated
514   kinase pathway in human schwannoma. Cancer Res. 2008;68:5236-45. DOI:10.1158/0008-
515   5472.CAN-07-5849

516   16. Zhou L, Ercolano E, Ammoun S, Schmid MC, Barczyk MA, Hanemann CO. Merlin-
517   deficient human tumors show loss of contact inhibition and activation of Wnt/β-catenin
518   signaling linked to the PDGFR/Src and Rac/PAK pathways. Neoplasia. 2011 Dec;13:1101-
519   12. DOI: 10.1593/neo.111060.

520   17. Provenzano L, Ryan Y, Hilton DA, Lyons-Rimmer J, Dave F, Maze EA, et al. Cellular
521   prion protein (PrPC) in the development of Merlin-deficient tumours. Oncogene.
522   2017;36:6132-42. DOI:10.1038/onc.2017.200

523   18. Adams CL; Ercolano E; Ferluga S; Sofela A; Dave F; Negroni C et al. A Rapid Robust
524   Method for Subgrouping Non-NF2 Meningiomas According to Genotype and Detection of
525   Lower Levels of M2 Macrophages in AKT1 E17K Mutated Tumours. Int J Mol Sci.
526   2020;21:1273. DOI:10.3390/ijms21041273

527 19. Kaempchen K, Mielke K, Utermark T, Langmesser S, Hanemann CO. Upregulation of the
528   Rac1/JNK signaling pathway in primary human schwannoma cells. Hum Mol Genet.
529   2003;12:1211-21. DOI:10.1093/hmg/ddg146

530 20. Théry C, Amigorena S, Raposo G, Clayton A. Isolation and characterization of exosomes
531   from cell culture supernatants and biological fluids. Curr Protoc Cell Biol. 2006;30: 3.22.1-
532   3.22.29. DOI:10.1002/0471143030.cb0322s30

533 21. Hanke K, Kramer P, Seeher S, Beimforde N, Kurth R, Bannert N. Reconstitution of the
534   ancestral glycoprotein of human endogenous retrovirus K and modulation of its functional
535   activity by truncation of the cytoplasmic domain. J Virol. 2009;83:12790-800.
536   DOI:10.1128/JVI.01368-09

537 22. Parkinson DB, Bhaskaran A, Arthur-Farraj P, Noon LA, Woodhoo A, Lloyd AC, et al. c-
538   Jun is a negative regulator of myelination. J Cell Biol. 2008;181:625-37. DOI:
539   10.1083/jcb.200803013.

540 23. Yue WY, Clark JJ, Fernando A, Domann F, Hansen MR. Contribution of persistent C-Jun
541   N-terminal kinase activity to the survival of human vestibular schwannoma cells by
542   suppression of accumulation of mitochondrial superoxides. Neuro Oncol. 2011;13:961-73.
543   DOI: 10.1093/neuonc/nor068.

544 24. Shivane A, Parkinson DB, Ammoun S, Hanemann CO. Expression of c-Jun and Sox-2 in
545   human schwannomas and traumatic neuromas. Histopathology. 2013;62:651-6.
546   DOI:10.1111/his.12062

547 25. Vargas A, Zhou S, Éthier-Chiasson M, Flipo D, Lafond J, Gilbert C, et al. Syncytin proteins
548   incorporated in placenta exosomes are important for cell uptake and show variation in
549   abundance in serum exosomes from patients with preeclampsia. FASEB J. 2014;28:3703-
550   19. DOI:10.1096/fj.13-239053

551 26. Manghera M, Ferguson-Parry J, Lin R, Douville RN. NF-κB and IRF1 Induce Endogenous
552   Retrovirus K Expression via Interferon-Stimulated Response Elements in Its 5' Long
553   Terminal Repeat. J Virol. 2016;90:9338-49. DOI:10.1128/JVI.01503-16

554 27. Li W, Cooper J, Zhou L, Yang C, Erdjument-Bromage H, Zagzag D, et al. Merlin/NF2
555   loss-driven tumorigenesis linked to CRL4(DCAF1)-mediated inhibition of the hippo
556   pathway kinases Lats1 and 2 in the nucleus. Cancer Cell. 2014;26:48-60.
557   DOI:10.1016/j.ccr.2014.05.001

558   28. Wang C, Zhu X, Feng W, Yu Y, Jeong K, Guo W, et al. Verteporfin inhibits YAP function
559   through up-regulating 14-3-3σ sequestering YAP in the cytoplasm. Am J Cancer Res.
560   2015;6:27-37.
561   29. Tang TT, Konradi AW, Feng Y, Peng X, Ma M, Li J, et al. Small Molecule Inhibitors of
562   TEAD Auto-palmitoylation Selectively Inhibit Proliferation and Tumor Growth of NF2-
563   deficient Mesothelioma. Mol Cancer Ther. 2021;20:986-998. DOI: 10.1158/1535-
564   7163.MCT-20-0717
565   30. Gatti G, Di Biagio A, Casazza R, De Pascalis C, Bassetti M, Cruciani M, et al. The
566   relationship between ritonavir plasma levels and side-effects: implications for therapeutic
567   drug monitoring. AIDS. 1999;13:2083-9. DOI:10.1097/00002030-199910220-00011
568   31. Kraus B, Boller K, Reuter A, Schnierle BS. Characterization of the human endogenous
569   retrovirus K Gag protein: identification of protease cleavage sites. Retrovirology.
570   2011;8:21. DOI:10.1186/1742-4690-8-21
571   32. Ruggieri A, Maldener E, Sauter M, Mueller-Lantzsch N, Meese E, Fackler OT, et al.
572   Human endogenous retrovirus HERV-K(HML-2) encodes a stable signal peptide with
573   biological properties distinct from Rec. Retrovirology. 2009;6:17. DOI:10.1186/1742-
574   4690-6-17
575   33. Zhu L, Liao S, Child M, Zhang J, Persson A, Sevinsky H, et al. Pharmacokinetics and
576   inhibitory quotient of atazanavir/ritonavir versus lopinavir/ritonavir in HIV-infected,
577   treatment-naive patients who participated in the CASTLE Study. J Antimicrob Chemother.
578   2012;67:465-8. DOI:10.1093/jac/dkr490
579   34. Rock BM, Hengel SM, Rock DA, Wienkers LC, Kunze KL. Characterization of ritonavir-
580   mediated inactivation of cytochrome P450 3A4. Mol Pharmacol. 2014;86:665-74.
581   DOI:10.1124/mol.114.094862
582   35. Ghassabian S, Rawling T, Zhou F, Doddareddy MR, Tattam BN, Hibbs DE, et al. Role of
583   human CYP3A4 in the biotransformation of sorafenib to its major oxidized metabolites.
584   Biochem Pharmacol. 2012;84:215-23. DOI:10.1016/j.bcp.2012.04.001
585   36. Dymond AW, So K, Martin P, Huang Y, Severin P, Mathews D, et al. Effects of
586   cytochrome P450 (CYP3A4 and CYP2C19) inhibition and induction on the exposure of
587   selumetinib, a MEK1/2 inhibitor, in healthy subjects: results from two clinical trials. Eur J
588   Clin Pharmacol. 2017;73:175-84. DOI:10.1007/s00228-016-2153-7

589   37. Ammoun S, Evans DG, Hilton DA, Streeter A, Hayward C, Hanemann CO. Phase 0 trial
590   investigating the intratumoural concentration and activity of sorafenib in neurofibromatosis
591   type 2. J Neurol Neurosurg Psychiatry. 2019;90:1184-87. DOI:10.1136/jnnp-2018-319713

592   38. Chow WA, Jiang C, Guan M. Anti-HIV drugs for cancer therapeutics: back to the future?.
593   Lancet Oncol. 2009;10:61-71. DOI:10.1016/S1470-2045(08)70334-6

594   39. Ahluwalia MS, Patton C, Stevens G, Tekautz T, Angelov L, Vogelbaum MA, et al. Phase
595   II trial of ritonavir/lopinavir in patients with progressive or recurrent high-grade gliomas. J
596   Neurooncol. 2011;102:317-21. DOI:10.1007/s11060-010-0325-3

597   40. Wang-Johanning F, Rycaj K, Plummer JB, Li M, Yin B, Frerich K, et al.
598   Immunotherapeutic potential of anti-human endogenous retrovirus-K envelope protein
599   antibodies in targeting breast tumors. J Natl Cancer Inst. 2012;104:189-210.
600   DOI:10.1093/jnci/djr540

601   41. Gehlhausen JR, Park SJ, Hickox AE, Shew M, Staser K, Rhodes SD, et al. A murine model
602   of neurofibromatosis type 2 that accurately phenocopies human schwannoma formation.
603   Hum Mol Genet. 2015;24:1-8. DOI: 10.1093/hmg/ddu414

604   42. Laurent N, de Boüard S, Guillamo J-S, Christov C, Zini R, Jouault H, et al. Effects of the
605   proteasome inhibitor ritonavir on glioma growth in vitro and in vivo. Mol Cancer Ther.
606   2004;3: 129–136.

607   43. Cherkasova E, Malinzak E, Rao S, Takahashi Y, Senchenko VN, Kudryavtseva AV, et al.
608   Inactivation of the von Hippel-Lindau tumor suppressor leads to selective expression of a
609   human endogenous retrovirus in kidney cancer. Oncogene. 2011;30:4697-706.
610   DOI:10.1038/onc.2011.179

611   44. Lamar JM, Xiao Y, Norton E, Jiang ZG, Gerhard GM, Kooner S, et al. SRC tyrosine kinase
612   activates the YAP/TAZ axis and thereby drives tumor growth and metastasis. J Biol Chem.
613   2019;294:2302-17. DOI:10.1074/jbc.RA118.004364

614   45. Ammoun S, Schmid MC, Zhou L, Ristic N, Ercolano E, Hilton DA, et al. Insulin-like
615   growth factor-binding protein-1 (IGFBP-1) regulates human schwannoma proliferation,
616   adhesion and survival. Oncogene. 2012;31:1710-22. DOI:10.1038/onc.2011.357

617   46. Manghera M, Douville RN. Endogenous retrovirus-K promoter: a landing strip for
618   inflammatory transcription factors? Retrovirology. 2013;10:16. DOI:10.1186/1742-4690-
619   10-16

620   47. Palmarini M, Maeda N, Murgia C, De-Fraja C, Hofacre A, Fan H. A phosphatidylinositol
621   3-kinase docking site in the cytoplasmic tail of the Jaagsiekte sheep retrovirus

transmembrane protein is essential for envelope-induced transformation of NIH 3T3 cells. J Virol. 2001;75:11002-9. DOI:10.1128/JVI.75.22.11002-11009.2001

48. Curty G, Marston JL, de Mulder Rougvie M, Leal FE, Nixon DF, Soares MA. Human Endogenous Retrovirus K in Cancer: A Potential Biomarker and Immunotherapeutic Target. Viruses. 2020;12:726. DOI: 10.3390/v12070726.

49. Dewannieux M, Blaise S, Heidmann T. Identification of a functional envelope protein from the HERV-K family of human endogenous retroviruses. J Virol. 2005;79:15573-7. DOI:10.1128/JVI.79.24.15573-15577.2005

50. Othman N, Jamal R, Abu N. Cancer-Derived Exosomes as Effectors of Key Inflammation-Related Players. Front Immunol. 2019;10:2103. DOI:10.3389/fimmu.2019.02103
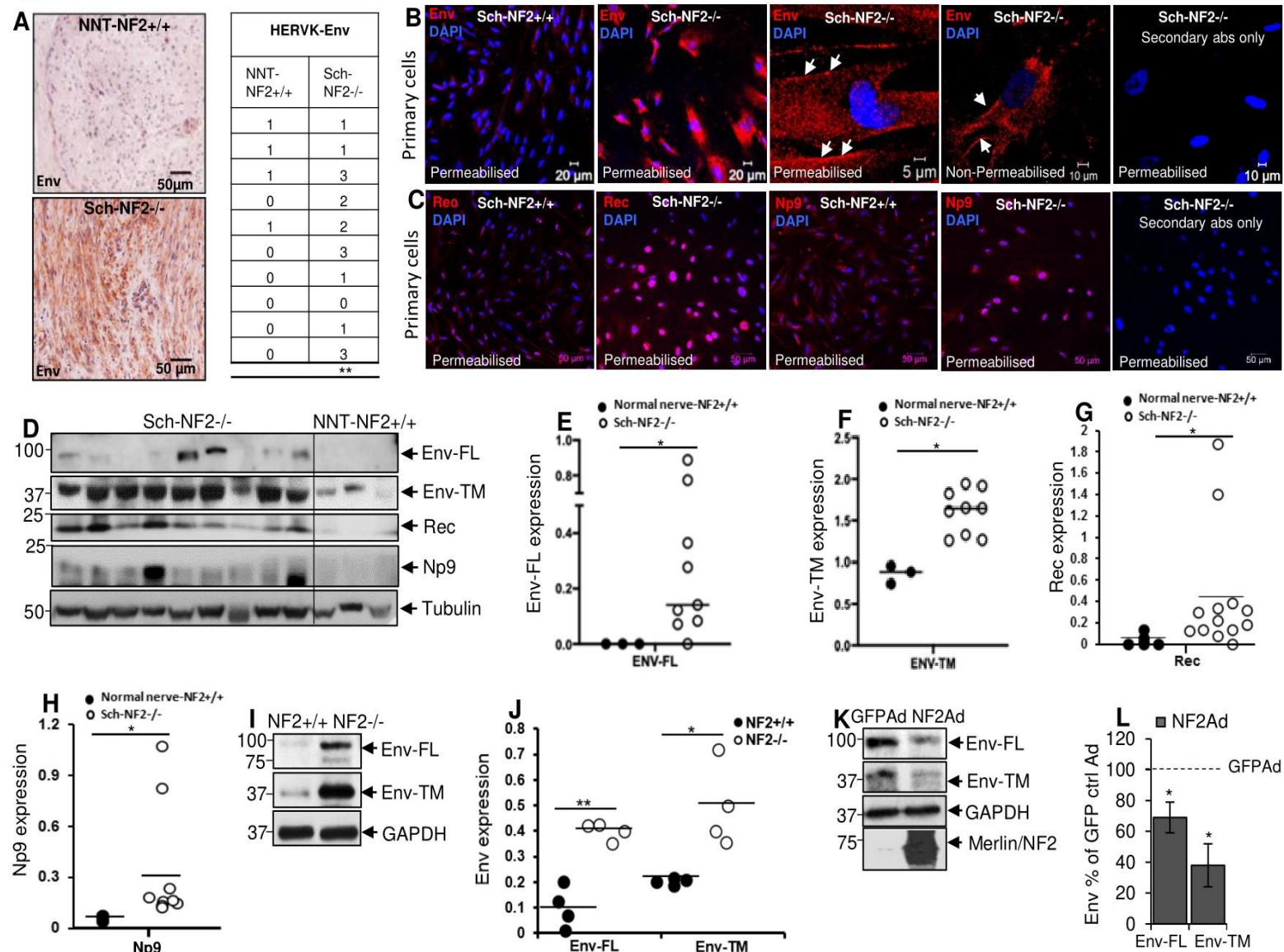
Figure 1

Figures

Figure 1. HERV-K-Env, Rec and Np9 proteins are overexpressed in Merlin-negative human primary schwannoma cells and tissues (Sch-NF2-/-). A, Representative IHC images showing negligible HERV-K-Env expression in normal nerve-NF2+/+ tissues (NNT-NF2+/+) compared to strong expression in Sch-NF2-/- tissues. Data are summarised in a table displaying staining intensity in samples from 10 patients and 10 healthy donors. **B,** Representative ICC images showing weak HERV-K Env ICC expression in Sch-NF2+/+ cells compared to strong cytoplasmic and membranous expression (white arrows) in both permeabilised and non-permeabilised Sch-NF2-/- cells. **C,** Representative ICC images showing strong Rec and Np9 nuclear expression in Sch-NF2-/- cells compared to Sch-NF2+/+ cells **(n=3). D-H,** WB (D) and quantifications (E-H) showing increased expression of HERV-K-Env (D, E, F; **n=9**), Rec (D, G; **n=13,** only representative n=9 samples are presented in figure D), and Np9 (D, H; **n=9**) in Sch-NF2-/- tissues compared to normal nerve-NF2+/+ tissues (**n=3 in D, n=5 in G**) detected by WB. **I, J** Representative WB showing precursor Env-FL and mature cleaved Env-TM detected by WB with stronger density in Sch-NF2-/- cells **(n=4)** compared to

Sch-NF2+/+ cells **(n=4)**. **K, L** Representative WB showing decreased Env-FL and Env-TM expression in Sch-NF2-/- cells after Merlin reintroduction using adenovirus vector (NF2Ad) compared to control adenovirus vector containing GFP only (GFPAd**)** (Env-FL, **n=7**; Env-TM, **n=4**). Secondary antibody only staining was used as a negative control in ICC (B, C). Tubulin (D) and GAPDH (I, K) were used as the loading control for WB.
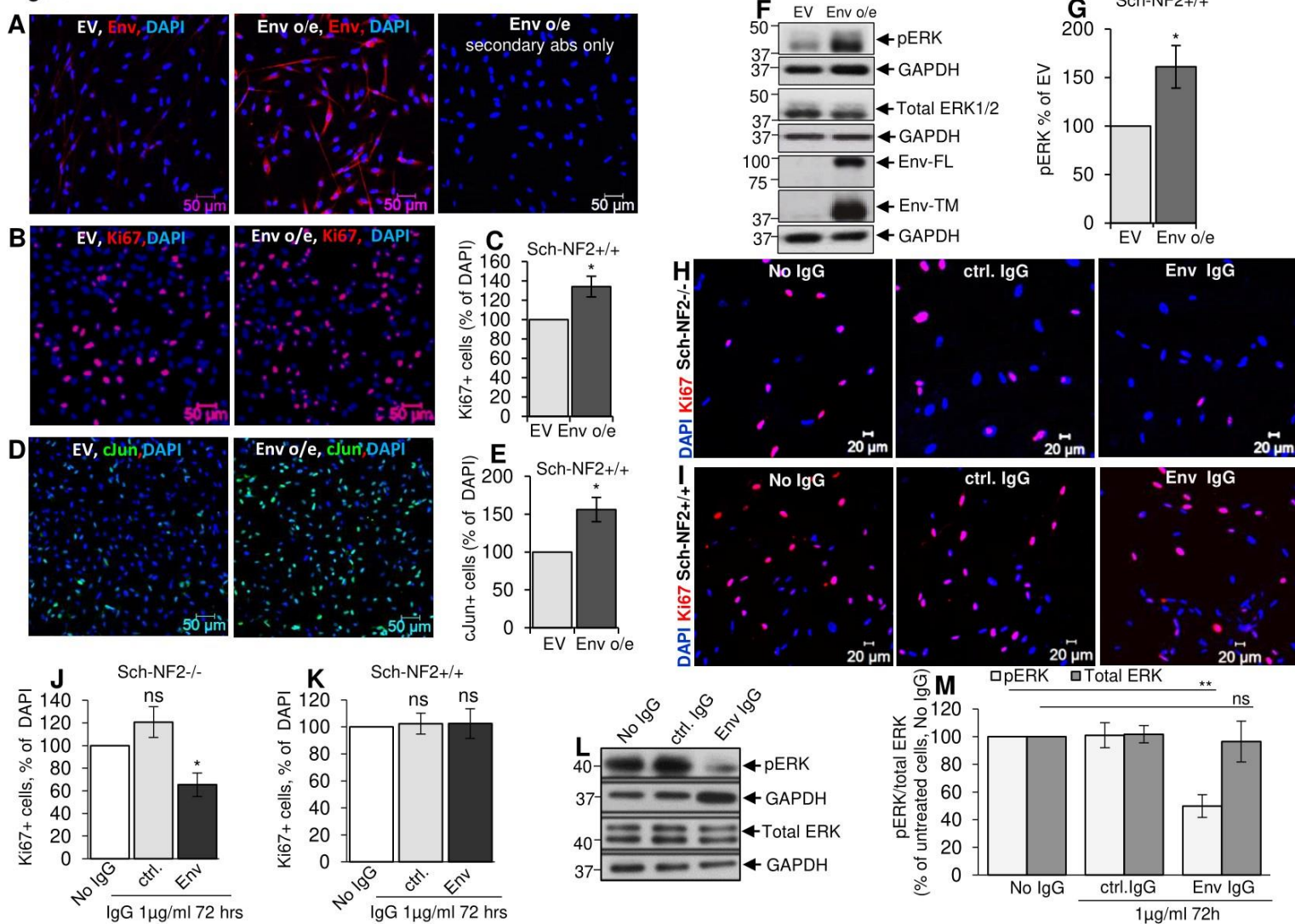
Figure 2. HERV-K-Env is involved in proliferation of Sch-NF2-/- cells via pERK. A-G, Representative immunocytochemistry for Env (red) shows ectopic overexpression of Env (Env o/e), compared to an empty vector (EV) control in Sch-NF2+/+ cells using lentiviral constructs (A), Env o/e increases number of Ki67 positive (red) cells compared to EV (B, C**; n=4)** and c-Jun (green)-expressing cells (D, E**; n=3),** and increases the levels of active pERK (F, G; **n=4). H-M,** Treatment with anti-HERV-K Env antibody decreases number of Ki67 positive cells in Sch-NF2-/- cells (H, J**; n=4**) but not in Sch-NF2+/+ cells (I, K**; n=3**). **L, M,** Anti-HERV-K Env antibody decreases the levels of active pERK in Sch-NF2-/- cells and has no effect on ERK expression. Staining using only the secondary antibody was used as a negative control in ICC, and GAPDH was used as a loading control for WB.

Figure 3
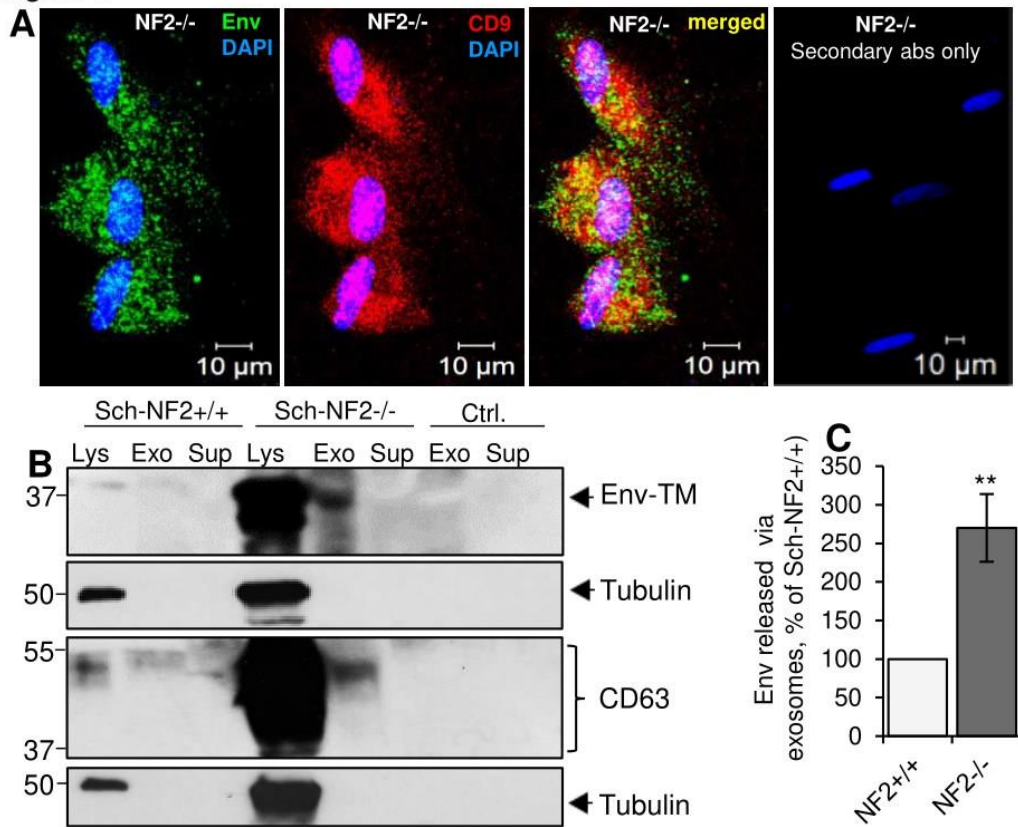
Figure 3. HERV-K-Env protein is released via exosomes. A, Representative immunocytochemistry (ICC) images show Env co-localisation with late endosome/exosome marker CD9 (red) in Sch-NF2-/- cells **(n=3)**. **B,** Representative western blot shows another late endosome/exosome marker CD63 on cell lysates (Lys, line 1) and exosome fractions (Exo, line 2) collected from cell culture medium after seven days of culture with Sch-NF2-/- cells, demonstrating the release of HERV-K Env-TM protein via exosomes **(n=5)**. Negative control (Ctrl.) is growth medium not exposed to the cells. **C,** The release of exosome-bound Env-TM is greater in Sch-NF2-/- cells compared to Sch-NF2+/+ cells. No Env protein was detected in exosome-free supernatant fractions (Sup, line 3) collected after exosome isolation (B, C). Tubulin was used as a loading control.

Figure 4
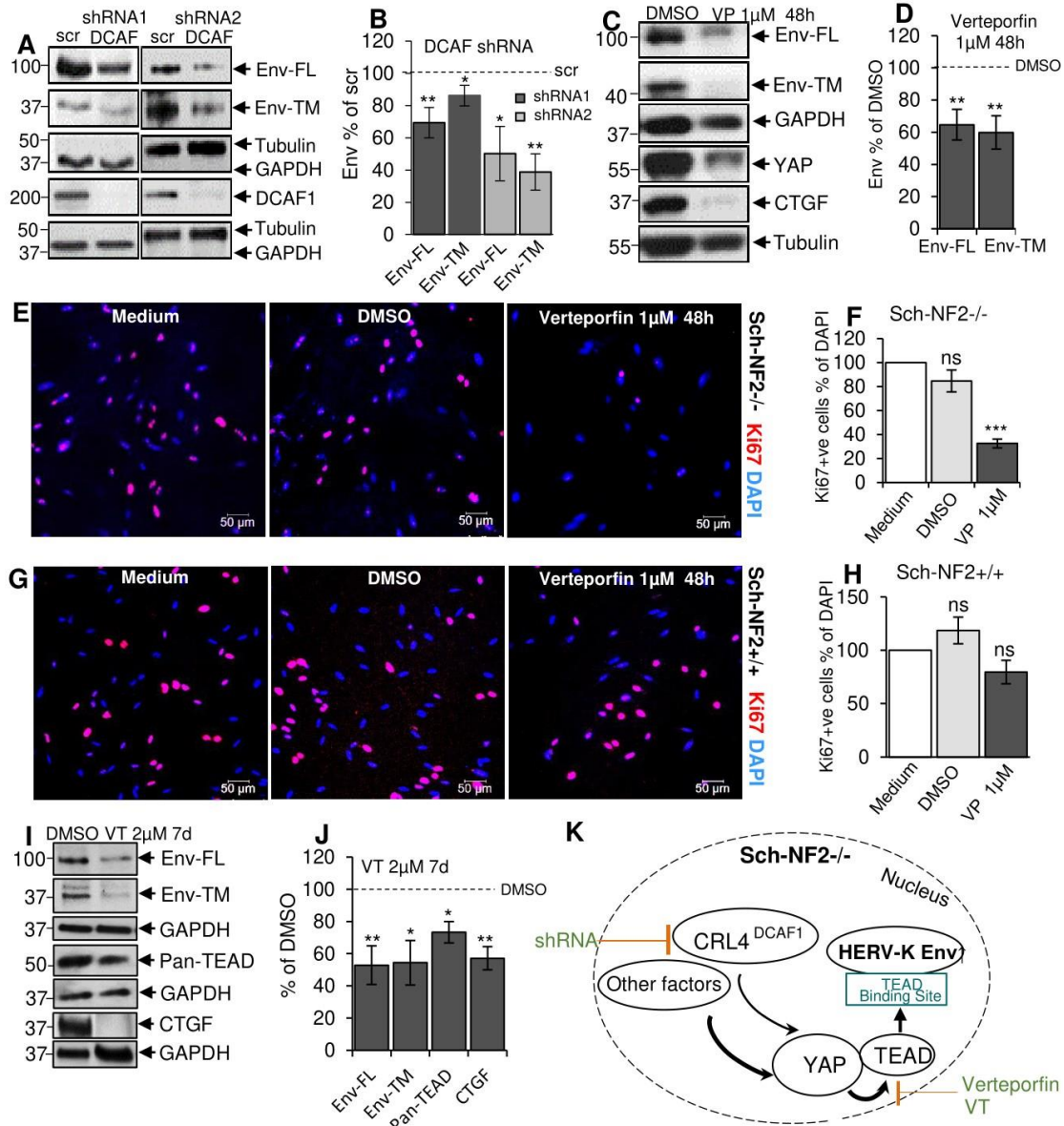
Figure 4. CRL4^DCAF1 and YAP/TEAD Hippo pathway is involved in the increased expression of HERV-K-Env in Sch-NF2-/- cells. A, B, Representative western blot showing that depletion of CRL4^DCAF1 by shRNA knockdown (shRNA 1 and shRNA 2) decreases expression of Env-FL **(n=4)** and Env-TM **(n=3)**. **C-H,** The YAP/TEAD inhibitor Verteporfin (VP) decreases expression of the HERV-K Env-FL **(n=5)** and Env-TM proteins (C, D; **n=4**), and reduces the number of Ki67 positive cells in Sch-NF2-/- cells (E, F; **n=3**) but not Sch-NF2+/+ cells (G, H; **n=3**). **I, J,** TEAD inhibitor VT107 (VT) strongly decreases expression of Env-FL **(n=4)** and Env-TM **(n=5)**. **K,** Schematic overview of the signalling pathways involved in increased expression of HERV-K Env. YAP, CTGF and pan-TEAD were used as positive controls for drug efficacy.

figure 5
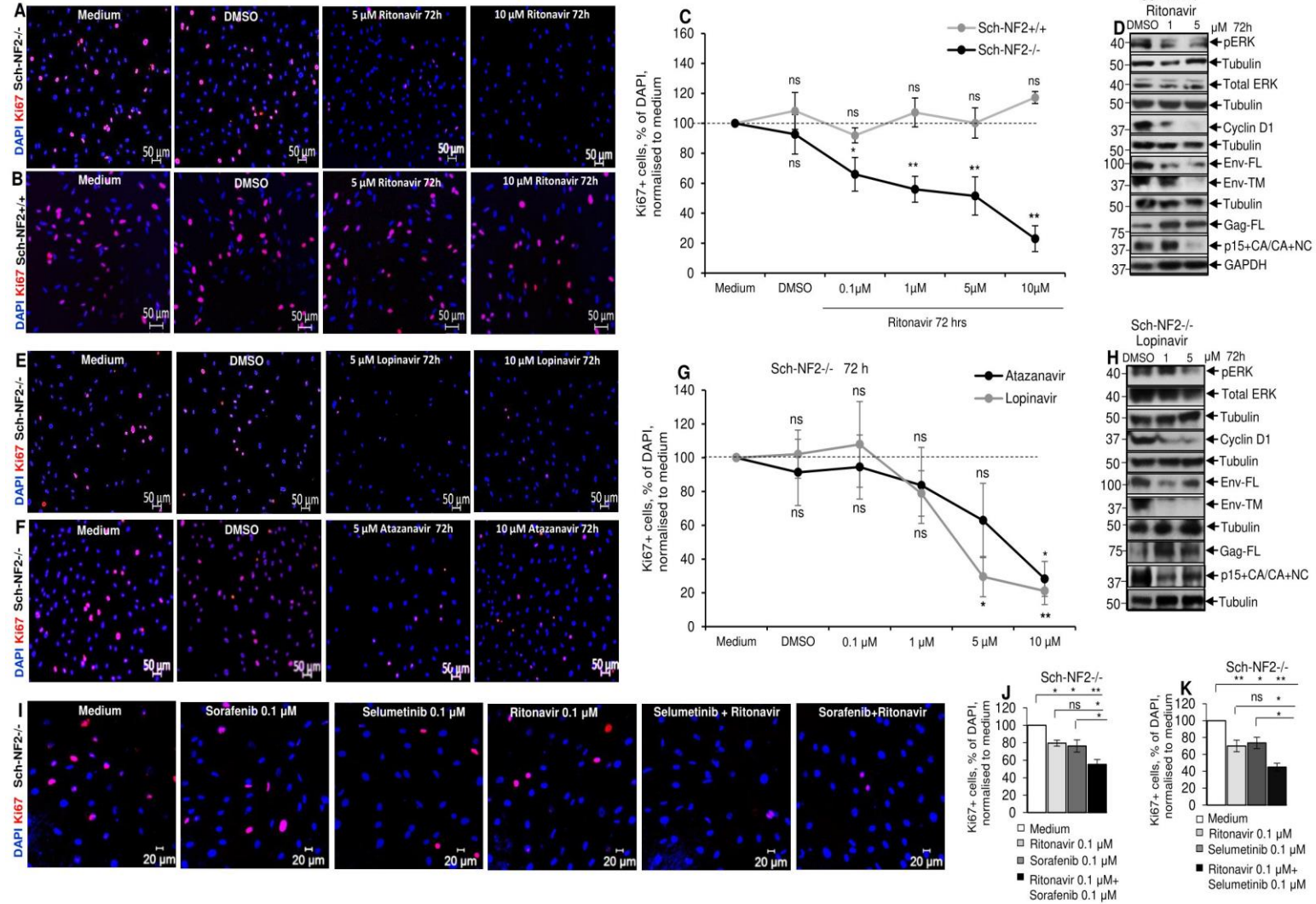
Figure 5. Anti-retroviral drug treatments in schwannoma cells (Sch-NF2-/-). A-C, Ritonavir strongly decreases proliferation (number of Ki67 positive cells) of Sch-NF2-/- (A, C; **n=8**) but not Sch-NF2+/+ cells (B, C**; n=5**). **D,** Ritonavir decreases levels of pERK **(n=5)**, cyclin D1 **(n=6)**, Env-FL **(n=5)** and Env-TM **(n=5)**. It also inhibits the HERV-K protease: increasing the level of uncleaved Gag-FL precursor protein and decreasing the level of cleaved p15+CA and/or CA+NC proteins **(n=10). E-G,** Lopinavir (E, G; **n=3)** and Atazanavir (F, G; **n=3**) decrease proliferation (number of Ki67 positive cells, Ki67+) of Sch-NF2-/- cells. **H,** Lopinavir decreases the levels of pERK **(n=5)**, cyclin D1 **(n=5)**, Env-FL **(n=4)** and Env-TM **(n=4)**. Lopinavir also inhibits the HERV-K protease: increasing the level of uncleaved Gag-FL **(n=3)** and decreasing the level of p15+CA and/or CA+NC **(n=4)**. **I-K,** Combined treatments of Sch-NF2-/- cells with Ritonavir + PDGFR/cRaf inhibitor Sorafenib **(n=7)** and Ritonavir + MEK1/2 inhibitor Selumetinib **(n=6).** GAPDH and tubulin were used as loading controls for WB.

33

Figure 6

Figure 6. HERV-K overexpression in Merlin-negative meningioma. A-G, WB demonstrating expression of Env-FL (A, D), Env-TM (A, E), Rec (B, F), and Np9 (C, G) in grade I Merlin-deficient meningioma biopsies (MN-GI-NF2-/-) **(n=14, n=14, n=10 and n=9** respectively**),** grade II Merlin-negative meningioma biopsies (MN-GII-NF2**-/-) (n=5, n=5; n=5 and n=4** respectively**),** and grade III Merlin-negative biopsies (MN-GIII-NF2-/-) **(n=3, n=3, n=2 and n=3** respectively**)** compared to normal meningeal tissues (NMT). **H, I,** WB demonstrating increased expression of Env-FL **(n=17)** but not Env-TM **(n=17)** in MN-GI-NF2-/- primary cells compared to normal human meningeal cells (HMC). **J, K,** Env-FL **(n=3)** and Env-TM **(n=4)** overexpression in MN-GI-NF2-/- cells is reversed by Merlin re-introduction (NF2-Ad). **L, M,** TEAD inhibitor VT107 decreases expression of Env-FL **(n=5)** and Env-TM **(n=5)** proteins. The specificity and efficiency of the drug was tested by measuring the expression of pan-TEAD and CTGF proteins. GAPDH and tubulin were used as loading controls for WB.

Figure 7
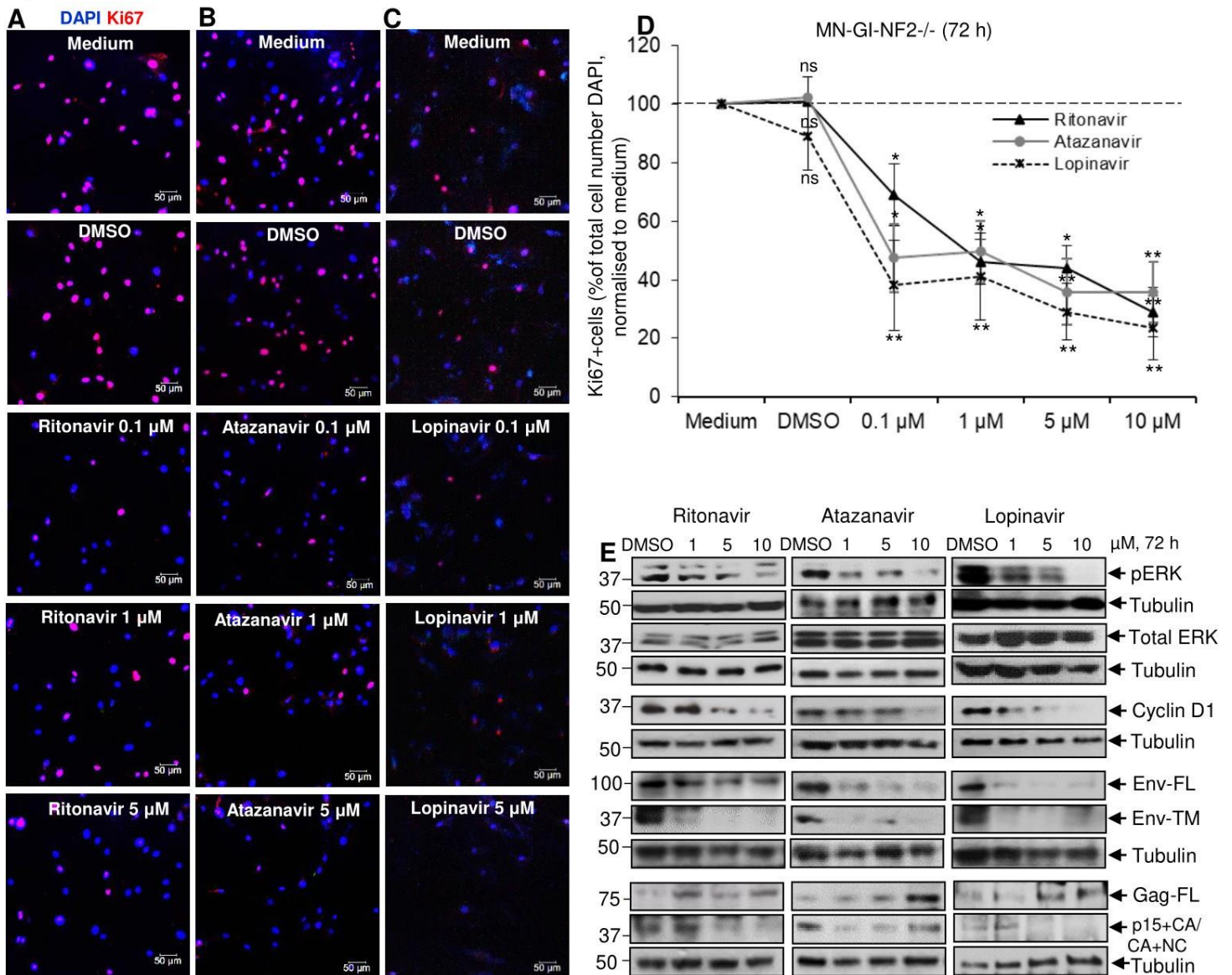
Figure 7. Ritonavir, Atazanavir and Lopinavir decrease proliferation of Merlin-negative grade I human meningioma primary cells (MN-GI-NF2-/-), inhibit HERV-K-Gag maturation and HERV-K-Env expression, and reduce the levels of active pERK and cyclin D1. A-D, Ritonavir (A, D; **n=7**), Atazanavir (B, D; **n=7**) and Lopinavir (C, D; **n=6**) decrease the number of Ki67 positive cells (Ki67+) in MN-GI-NF2-/- primary cells. **E,** Ritonavir, Atazanavir and Lopinavir decrease the levels of pERK (but not total ERK) (**n=6, n=6 and n=8** respectively), cyclin D1 (**n=6, n=7 and n=7** respectively), HERV-K-Env (both FL and TM) (**n=6, n=5 and n=6** respectively), and inhibit maturation of HERV-K Gag (increasing Gag-FL and decreasing p15+CA/CA+NC levels) (**n=4, n=7 and n=7** respectively). Tubulin was used as a loading control for WB.

632

Supplementary data

Supplementary figure 1
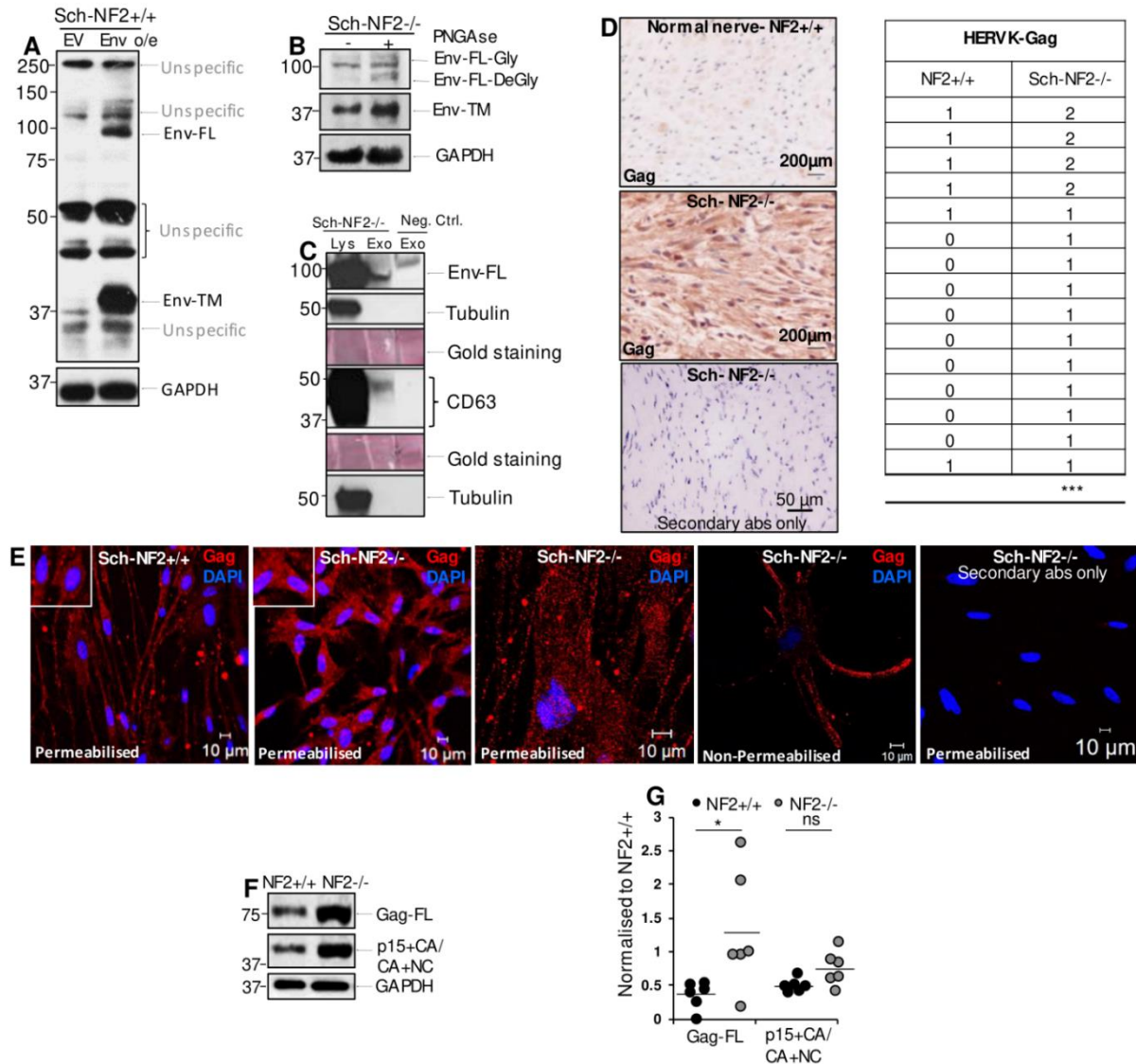
Supplementary figure S1. A, Western blot picture demonstrating different bands detected with the anti-HERV Env antibody in normal Merlin-positive (NF2+/+) human primary Schwann cells (Sch-NF2+/+) transduced with either empty vector (EV) or with HERV-K Env containing vector (Env o/e) **(n=4). B,** Western blot demonstrating molecular weight shift of Env-FL band in Merlin-deficient (NF2-/-) human primary schwannoma cells (Sch-NF2-/-) after treatment with PNGAse **(n=3). C,** Western blot picture demonstrating band for Env-FL in cell lysate, and co-migrating bands in exosomes isolated from cell culture media from Sch-NF2-/- cells and control media not exposed to cells (Neg. ctrl). **D,** IHC staining with anti-HERV-K Gag antibody in normal nerve-NF2+/+ and Sch-NF2-/- tissues and staining without primary antibody (secondary abs only) in Sch-NF2-/- tissue (left panel). Table summarising the expression of HERV-K Gag in normal nerve-NF2+/+ tissues compared to Sch-NF2-/- tissues (right panel, scoring as in fig. 6B). **E,** ICC staining with anti-HERV-K Gag antibody in permeabilised Sch-NF2+/+ and in permeabilised and non-permeabilised Sch-NF2-/- cells, and control staining using only the secondary antibody **(n=3). F, G,** HERV-K Gag-FL and p15+CA/CA+NC expression in Sch-NF2-/- cells **(n=6)** compared to Sch-NF2+/+ cells **(n=6).**

Supplementary figure 2
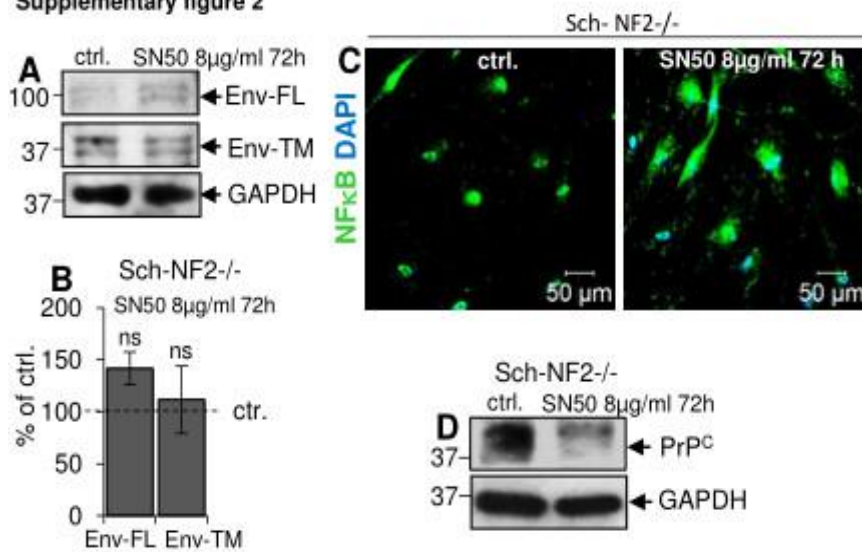
Supplementary figure S2. A, B, Western blot image (A) and bar chart (B) demonstrating the expression of HERV-K Env-FL and Env-TM before and after treatment with NFκB inhibitor SN50 **(n=3)**. **C,** ICC staining with anti-NFκB antibody before and after treatment of Sch-NF2-/- cells with SN50 **(n=3)**. **D,** Western blot demonstrating the effect of SN50 on the expression of cellular prion protein PrP^C, used as a positive control for drug activity **(n=3).**

Supplementary figure 3

1 NFκB (61-70)	**4** NFAT-1 (568-572) / NFκB (568-579)	**7** Oct4 (691-701)
2 YY1 (62-83)	**5** GC box 1 (575-579)	**8** GC box 3 (762-766)
3 TEAD (518-524) / NFκB (519-528)	**6** GC box 2 (602-606)	**9** GC box 4 (820-824)
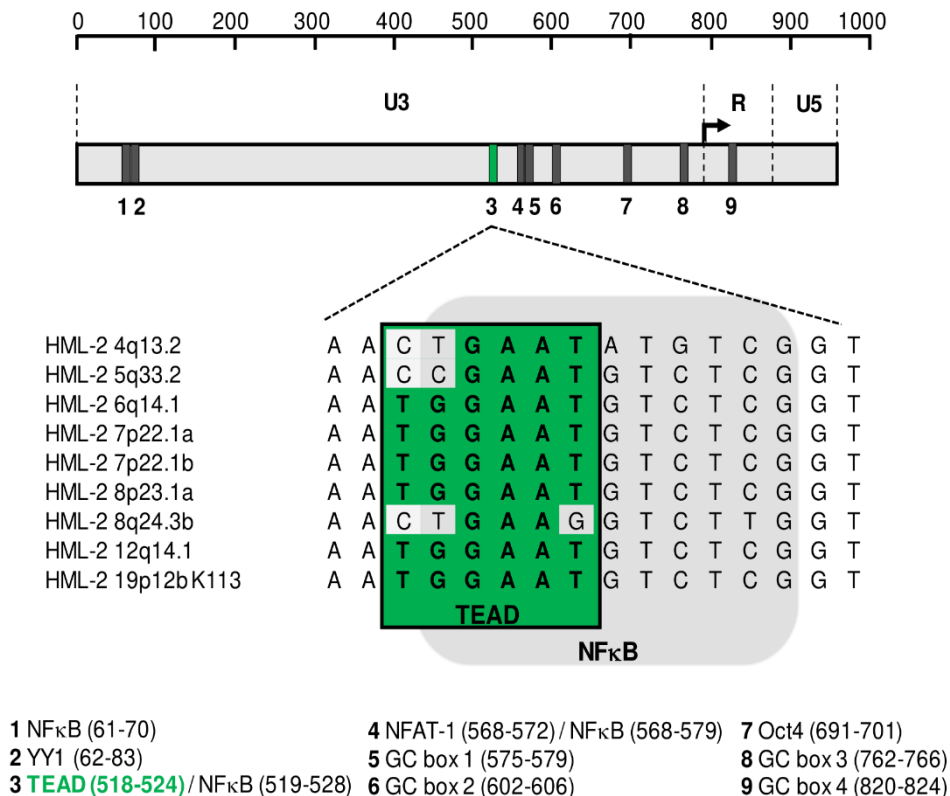
Supplementary figure S3. Locations of transcription factors binding sites on HERV-K LTR experimentally assessed are represented. Location of a potential binding site for TEAD identified in this study is also represented along with motif conservation across HERV-K proviruses that harbour full LTR and *env* ORF sequences (Subramanian et al. 2011, PMID: 22067224). Note TEAD's putative

binding motifs TGGAAT (Vassilev et al. 2001, PMID: 11358867), sharing binding site with NFκB, as previously reported (Sawada et al., 2005, PMID: 16207754).

Supplementary figure 4
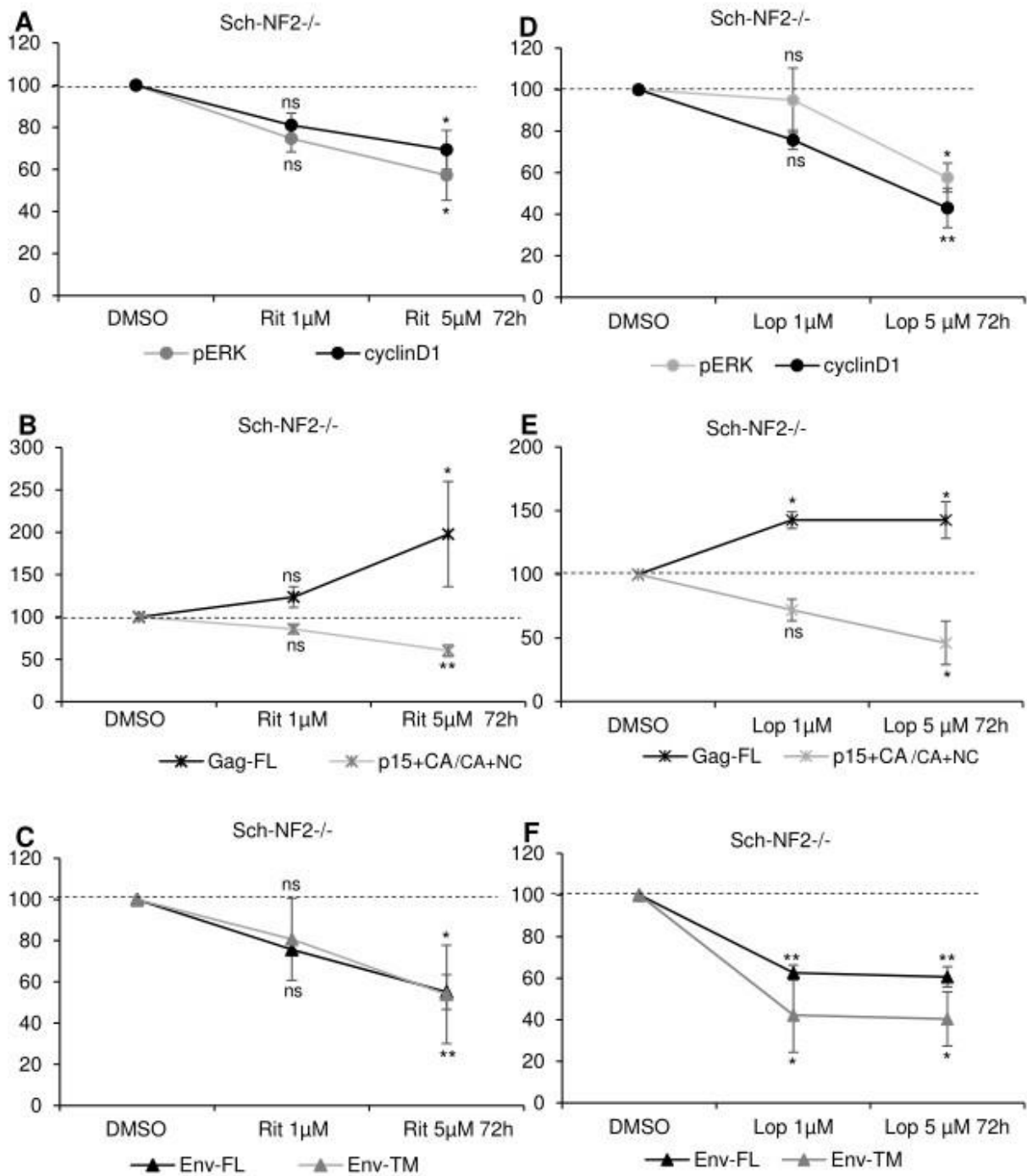
Supplementary figure S4. A-F, Graphs demonstrating the effect of Ritonavir (Rit) (A, B, C) and Lopinavir (Lop) (D, E, F) on levels of pERK, cyclin D1, HERV-K Env (FL and TM) and Gag (FL, p15+CA/CA+NC) in Sch-NF2-/- cells.

Supplementary figure 5

A NMT | MN-GI-NF2-/- | MN-GI-NF2-/- | MN-GII-NF2-/- | MN-GIII-NF2-/-

100 — ← Gag-FL
40 — ← p15+CA/CA+NC
50 — ← Tubulin

D MN-GI-NF2-/- | HMC

100 — ← Gag-FL
40 — ← p15+CA/CA+NC
37 — ← GAPDH

B
- NMT ○ G-I ● G-II/III

Gag-FL
ns   ns

C
- NMT ○ G-I ● G-II/III

p15+CA/CA+NC
*   ns

E
● HMC ● G-I

Gag-FL
*

F
● HMC ● G-I

p15+CA/CA+NC
ns

G

NMT — Meninges / Brain — Env — 50µm
MN-GI — Env
MN-GII — Env
MN-GIII — Env

H

NMT — Meninges / Brain — Gag — 50µm
MN-GI — Gag
MN-GII — Gag
MN-GIII — Gag

I

HERV-K Env			
NMT	G-I	G-II	G-III
2	2 NF2-/-	2 ND	3 ND
1	2 NF2-/-	3 ND	3 NF2-/-
2	2 NF2-/-	2 ND	3 ND
1	3 NF2-/-	3 NF2-/-	3 NF2-/-
0	3 NF2-/-	2 ND	2 ND
0	2 NF2-/-	2 ND	3 ND
1	2 NF2-/-	3 ND	3 ND
1	3 NF2-/-	2 NF2-/-	3 ND
1			3 ND
2			

** / ** / ***
ns / *
ns

J

HERV-K Gag			
NMT	G-I	G-II	G-III
2	2 NF2-/-	1 ND	2 ND
0	2 NF2-/-	1 ND	2 NF2-/-
1	2 NF2-/-	1 ND	2 ND
1	2 NF2-/-	1 NF2-/-	2 NF2-/-
1	3 NF2-/-	1 ND	2 ND
1	2 NF2-/-	1 ND	1 ND
2	3 NF2-/-	2 ND	2 ND
1	3 NF2-/-	2 NF2-/-	1 ND
1			1 ND
1			

** / ns / ns
** / *
ns

K HMC
EV | Env o/e

100 —
75 — ← Env-FL
← Unspecific
50 —
37 — } Env-TM
25 —
50 — ← Tubulin

L
Env DAPI — CD63 DAPI — merged — merged
50 µm — 50 µm — 50 µm — 20 µm

M HMC | MN-GI-NF2-/- | HMC MN
Ctrl. Media
Lys Exo Sup | Lys Exo Sup | Exo Exo
Media | Media

100 — ← Env-FL
37 — ← Env-TM
50 — ← Tubulin
Gold staining
50 — CD63
37 —
50 — ← Tubulin
Gold staining

Supplementary figure S5. A-C, Western blot demonstrating the expression of HERV-K-Gag-FL (A, B) and HERV-K-p15+CA/CA+NC (A, C) in Merlin negative (NF2-/-) grades I-III meningioma tissues, MN-GI-NF2-/- **(n=9),** MN-GII-NF2-/- **(n=6)** and MN-GIII-NF2-/- **(n=2),** compared to normal meningeal tissues (NMT). **D-F,** Western blot demonstrating the expression of HERV-K-Gag-FL (D, E) and HERV-K-p15+CA/CA+NC (D, F) in MN-GI-NF2-/- primary cells **(n=8)** compared to normal meningeal cells (HMC). **G, H**, IHC staining for HERVK-Env and HERV-K-Gag in NMT, MN-GI, MN-GII, and MN-GIII meningioma tissues. **I, J,** Tables summarising the expression of HERVK-Env and HERV-K Gag in NMT and grades I-III meningioma tissues. Merlin status is given as Merlin-negative (NF2-/-) or not determined ND. **K,** Western blot demonstrating different bands detected with the anti-HERV-K Env antibody in HMC transduced with either empty vector (EV) or HERV-K Env-containing vector (Env o/e) **(n=3)**. **L,** ICC demonstrates cytoplasmic and membranous HERV-K Env localisation in MN-GI-NF2-/- cells (white arrows) and partial intracellular co-localisation of Env with late endosome/exosome marker CD63 **(n=3)**. **M,** Western blot of exosome fractions collected from cell culture medium after seven days with MN-GI-NF2-/- cells does not show any release of HERV-K Env proteins via exosomes **(n=3)**. The band in the exosome fraction detected at the molecular weight corresponding to Env-FL is not specific – a similar sized band was detected in the exosome fraction of the negative control (growth medium not exposed to cells). Negative control (Ctrl. Media) is growth medium not exposed to the cells.

Supplementary Figure 6
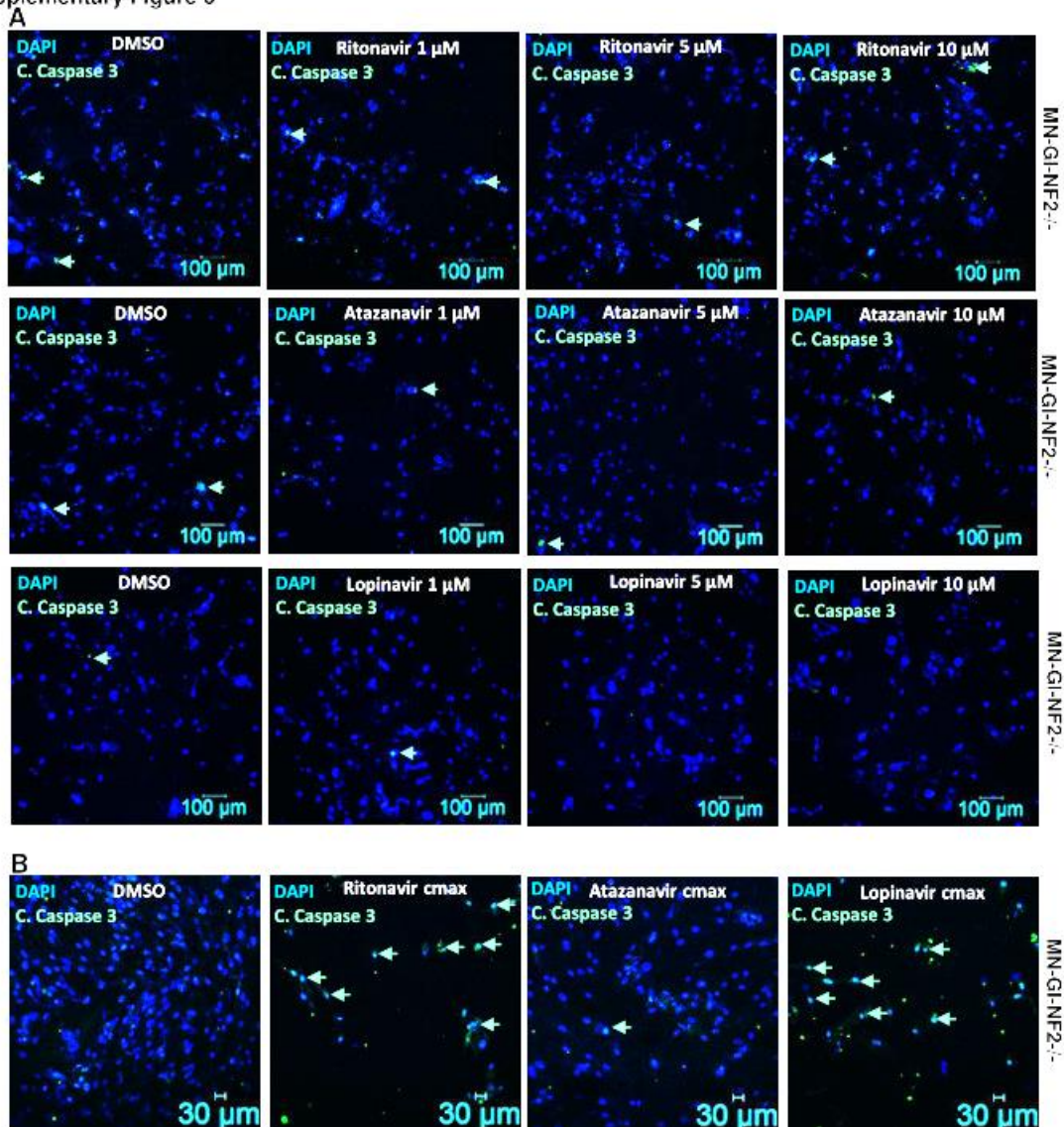
Supplementary figure S6. A, ICC pictures demonstrating that 72 hours treatment of MN-GI-NF2-/- cells with Ritonavir, Atazanavir and Lopinavir at concentrations of 1 µM, 5 µM and 10 µM, is not inducing cell death. **B,** Ritonavir and Lopinavir, but not, Atazanavir, lead to almost 100% cell death when used at cmax plasma concentrations (Ritonavir 22 µM, Lopinavir 17 µM and Atazanavir 4.1 µM) for 72 hours. Cleaved (C.) Caspase 3 (Green) is marker for apoptosis and DAPI (Blue) is used as nuclear marker. Experiments were performed in primary cells from n=3 different patients.

Supplementary figure 7
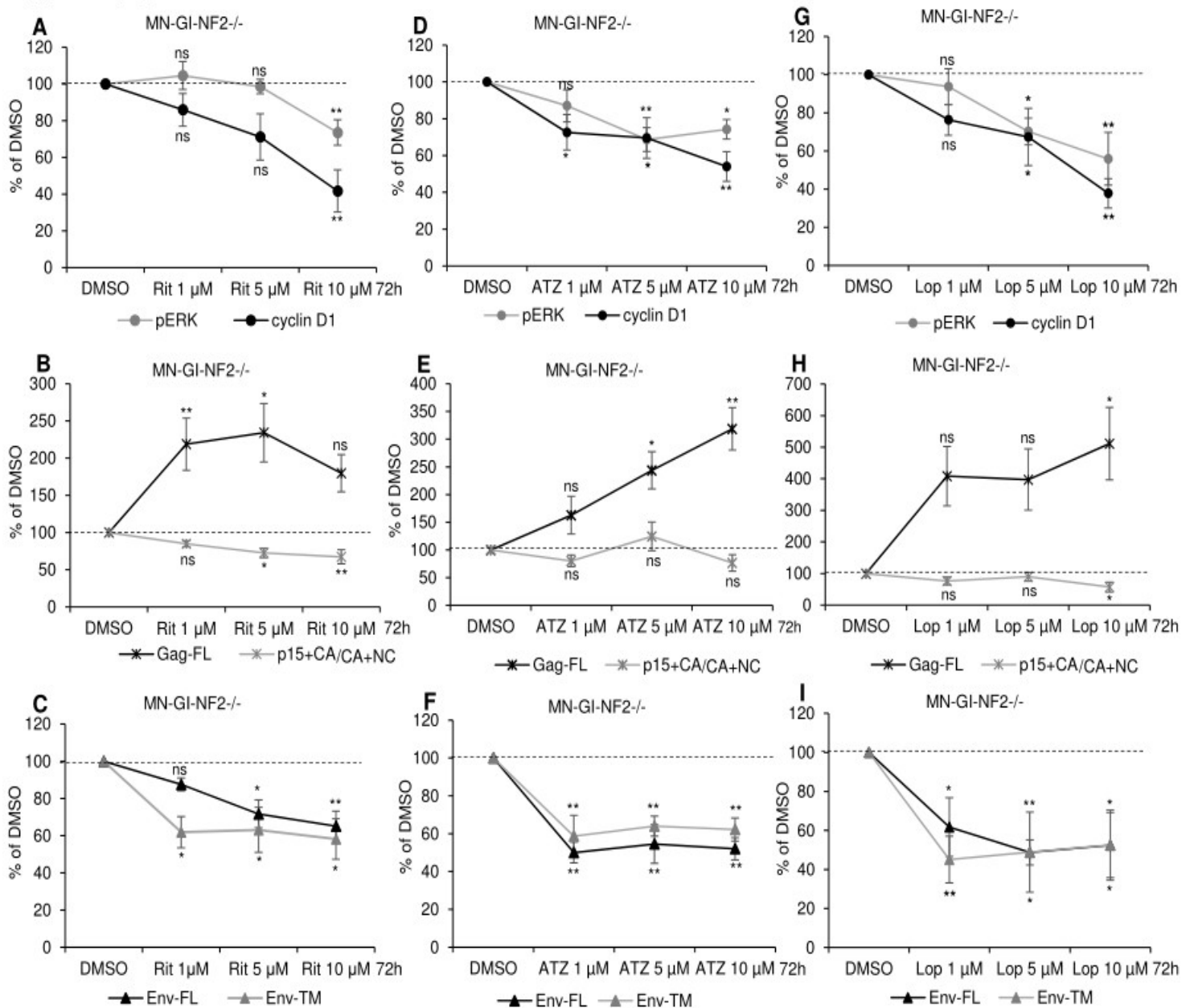
Supplementary figure S7. A-I, Graphs demonstrating the effect of Ritonavir (Rit) (A, B, C), Atazanavir (ATZ) (D, E, F)) and Lopinavir (Lop) (G, H, I) on the levels of pERK, cyclin D1, HERV-K Env (FL and TM) and Gag (FL and p15+CA/CA+NC) in MN-GI-NF2-/- cells.

633

Schwannoma									
No.	Site	Age/Gender	Grade	NF2	No.	Site	Age/Gender	Grade	NF2
1	NR	NR/NR	I	-/-	15	VS	45/F	I	-/-
2	CPA	43/F	I	-/-	16	VS	65/F	I	-/-
3	VS	69/M	I	-/-	17	VS	56/M	I	-/-
4	VS	70/F	I	-/-	18	VS	52/M	I	-/-
5	VS	46/M	I	-/-	19	VS	NR/NR	I	-/-
6	NR	NR	I	-/-	20	VS	28/M	I	-/-
7	VS	27/M	I	-/-	21	VS	46/M	I	-/-
8	VS	53/M	I	-/-	22	NR	NR/NR	I	-/-
9	NR	NR/NR	I	-/-	23	NR	NR/NR	I	-/-
10	VS	59/F	I	-/-	24	NR	NR/NR	I	-/-
11	C	30/F	I	-/-	25	NR	NR/NR	I	-/-
12	VS	59/F	I	-/-	26	NR	NR/NR	I	-/-
13	VS	44/F	I	-/-	27	NR	NR/NR	I	-/-
14	VS	62/M	I	-/-	NR=Not reported VS=Vestibular schwannoma C=Cervical CPA=Cerebellopontine angle				

Supplementary table S1. Patient information-Schwannoma.

Meningioma											
No.	Type	Site	Age/Gender	Grade	NF2	No.	Type	Site	Age/Gender	Grade	NF2
1	P	Spinal	NR/F	I	-/-	29	T	Frontal	73/F	I	-/-
2	M	Spinal	48/NR	I	-/-	30	M	Petroclivar	37/F	I	-/-
3	T	Sphenoid	66/F	I	-/-	31	T	Sphenoid	41/F	I	-/-
4	M	Middle Fossa	56/F	I	-/-	32	T	Parasagittal	37/F	I	-/-
5	T	Parasagittal	50/F	I	-/-	33	At	Occipital	66/M	II	-/-
6	F	Intra-ventricular	56/F	I	-/-	34	At	Temporal	NR/F	II	-/-
7	T	Parasagittal	42/M	I	-/-	35	At	Sub-frontal	NR/NR	II	-/-
8	T	Trigonal	NR/NR	I	-/-	36	At	Frontal	50/M	**II**	-/-
9	F	Frontal	80/F	I	-/-	37	At	Parietal	59/M	II	-/-
10	F	Occipital	50/F	I	-/-	38	At	Frontal	80/M	II	-/-
11	T	Frontal	51/F	I	-/-	39	At	Frontal	49/M	II	ND
12	T	Spinal	63/F	I	-/-	40	At	Frontal	71/F	II	ND
13	T	Thoracic	72/F	I	-/-	41	At	Frontal	66/M	II	ND
14	NR	Middle Fossa	62/F	I	-/-	42	At	Posterior fossa	71/M	II	ND
15	T	Frontal	35/F	I	-/-	43	At	Frontal	49/M	II	ND
16	T	Frontal	56/F	I	-/-	44	At	Parietal	66/M	II	ND
17	F	Post fossa	33/F	I	-/-	45	An	Frontal	77/M	III	ND
18	F	Parasagittal	74/M	I	-/-	46	An	Frontal	76/F	III	ND
19	T	Parasagittal	NR/F	I	-/-	47	An	Frontal	75/F	III	ND
20	NR	NR	NR	I	-/-	48	An	Frontal	70/M	III	ND
21	P	NR	NR/NR	I	-/-	49	An	Frontal	71/M	III	ND
22	T	Frontal	35/F	I	-/-	50	An	Frontal	41/M	III	ND
23	T	NR	NR/NR	I	-/-	51	An	NR	NR/NR	III	ND
24	F	Frontal	70/F	I	-/-	52	An	Occipital	85/M	III	-/-
25	P	Spinal	NR/F	I	-/-	53	R/Ang/Mi	Parietal	34/M	III	-/-
26	T	Parasagittal	53/M	I	-/-	54	An	Temporal	62/M	III	-/-
27	P	Occipital	64/F	I	-/-	At=Atypical ; Ang=Angiomatous; An=Anaplastic; F=Fibroblastic; M=Meningothelial; Mi=Microcytic; P=Psammomatous ; R=Rhabdoid; T=Transitional; ND=Not Determined; NR=Not Reported					
28	NR	Middle Fossa	62/F	I	-/-						

Supplementary table S2. Patient information-Meningioma.

IC50 uM	Ritonavir		Atazanavir		Lopinavir	
	IC50	95% CI	IC50	95% CI	IC50	95% CI
pERK	1.35	[0.34; 7.83]	ND	ND	1.26	[0.82; 1.78]
Cyclin D1	2.31	[0.87; 7.03]	ND	ND	0.76	[0.29; 1.39]
Env-FL	1.23	[0.74; 2.37]	ND	ND	incalculable	incalculable
Env-TM	0.55	$[2 \times 10^{-4}; 0.87]$	ND	ND	8.78×10^{-3}	$[1.6 \times 10^{-5}; 7.9 \times 10^{4}]$
P15+CA/CA +NC	1.31	[0.78; 2.34]	ND	ND	1.38	[0.25; 136.78]
Ki67	2.9	$[7.3 \times 10^{-5}; 9.08]$	7.38	[2.26; 10.09]	3.66	[1.3; 6.56]

Supplementary table S3. Table summarising the efficacy of Ritonavir and Lopinavir in decreasing proliferation (Ki67) and signalling pathways in Sch-NF2-/- cells**.**